Annual Report

# Electrooptical Devices

30 September 1983

Lincoln Laboratory

MASSACHUSETTS INSTITUTE OF TECHNOLOGY

LEXINGTON, MASSACHUSETTS

ADA197070

This technical report has been reviewed and is approved for publication.

FOR THE COMMANDER

Hugh L. Southall

Hugh L. Southall, Lt. Col., USAF
Chief, ESD Lincoln Laboratory Project Office

MASSACHUSETTS INSTITUTE OF TECHNOLOGY
LINCOLN LABORATORY

ELECTROOPTICAL DEVICES

ANNUAL REPORT
TO THE
ROME AIR DEVELOPMENT CENTER

1 OCTOBER 1982 — 30 SEPTEMBER 1983

ISSUED 25 APRIL 1988

LEXINGTON   MASSACHUSETTS
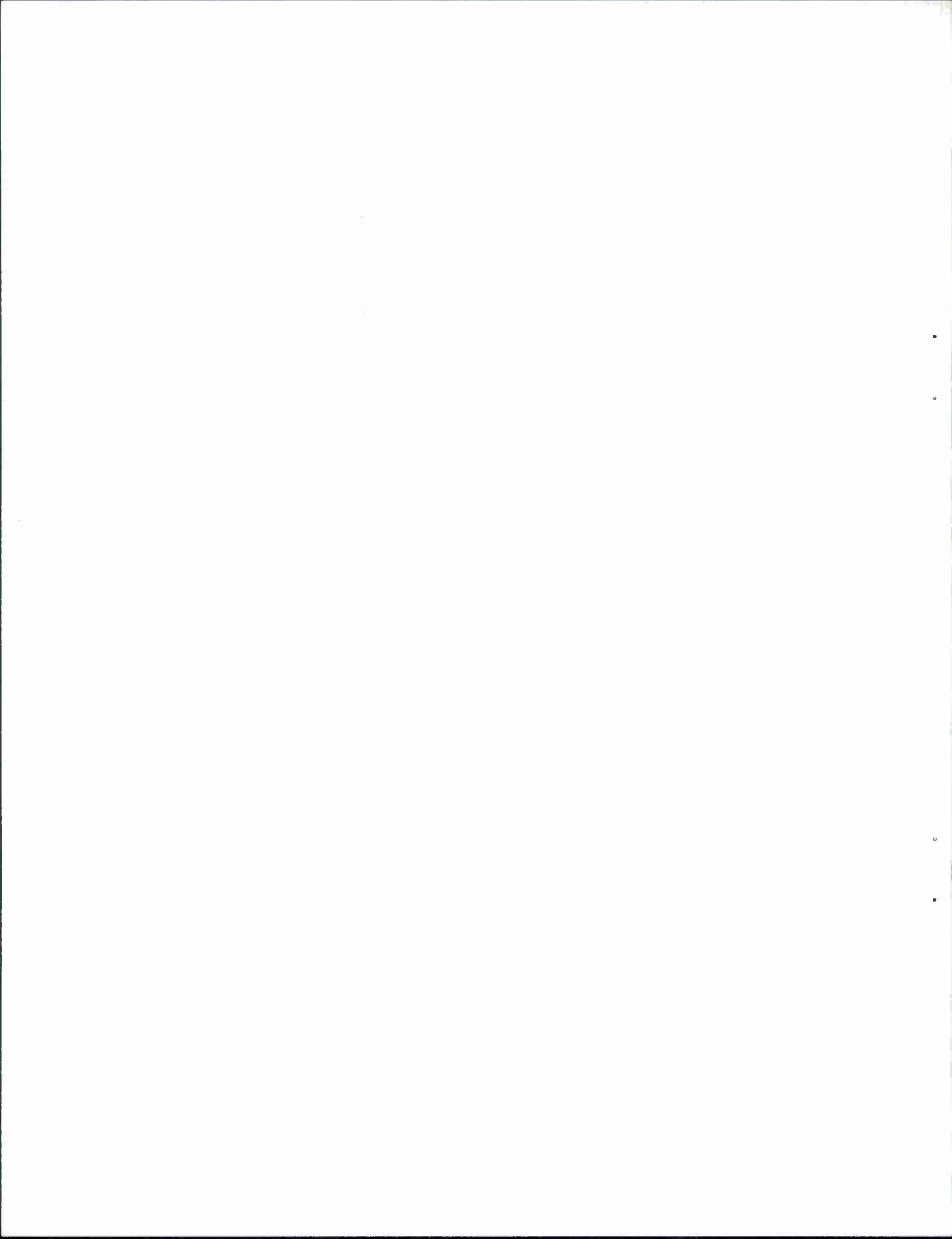
ABSTRACT

This report covers work carried out with the support of the Rome Air Development Center during the period 1 October 1982 through 30 September 1983.

A mass-transport phenomenon has been utilized to achieve GaInAsP/InP buried-heterostructure (BH) lasers. This novel technique is considerably simpler and more easily controlled than those previously reported, and has resulted in BH lasers with threshold currents as low as 9.0 mA.

The technology for fabricating laser diodes, detectors, and optical waveguides in GaInAsP/InP epitaxial wafers requires the use of suitable etching techniques for providing smooth, damage-free surfaces for precision pattern geometries and for the preferential and reproducible removal of specific layers. It has been found that a 1 H_2SO_4:1 H_2O_2:10 H_2O room-temperature solution etches (100) $Ga_{0.27}In_{0.73}As_{0.03}P_{0.37}$ (λ = 1.3 μm) at a very constant etch rate of 1000 Å/min. Other ratios of H_2SO_4:H_2O_2:H_2O should prove useful as slow selective etches for GaInAsP in a variety of applications.

Three-guide optical couplers consisting of slab-coupled rib-type guides have been fabricated on GaAs. Their behavior closely approximates that predicted using an effective-index analytic method. Couplers of this type should prove useful as replacements for "Y"-type power dividers and combiners, especially in cases where waveguide bends would result in unacceptable losses.

GaInAsP diode lasers with a proton-isolated modulator have been operated with full on/off modulation at rates of 3 GHz. Both the gain and loss are actively varied in the modulator in order to Q-switch the laser.

TABLE OF CONTENTS

LIST OF ILLUSTRATIONS

ELECTROOPTICAL DEVICES

I. A NOVEL TECHNIQUE FOR GaInAsP/InP
BURIED-HETEROSTRUCTURE LASER FABRICATION

A novel technique for the fabrication of GaInAsP/InP buried-heterostructure (BH) lasers has been developed. It is based on a mass-transport phenomenon which was recently observed during the fabrication of integrated laser-waveguide structures.[1] This technique is considerably simpler and more easily controlled than those previously reported,[2-15] and has resulted in BH lasers with threshold currents as low as 9.0 mA.

The experimental procedure is illustrated in Figure I-1(a) to (c). The starting wafer [a double-heterostructure (DH) wafer] was prepared by conventional liquid-phase-epitaxial (LPE) techniques on a (100) InP substrate. (Broad-area lasers fabricated from similar wafers have had threshold current densities of 0.9 to 1.3 kA/cm^2.) Oxide-stripe masks 5.0 to 6.0-μm-wide on 250-μm centers were first fabricated on the wafer, with the stripes parallel to either (011) or (011) crystallographic directions. Two steps of selective chemical etching were used in order to produce the mesa structure shown in Figure I-1(b). First, concentrated HCl was used to remove the unprotected InP cap layer. The $Ga_{0.27}In_{0.73}As_{0.63}P_{0.37}$ active layer thus exposed was then removed with a 50-ml aqueous solution of 10 g KOH and 0.2 g $K_3Fe(CN)_6$. Etching, beyond that required to remove the quaternary layer, was sometimes used, depending on the desired amount of undercutting [Figure I-1(b)].

After completion of the etching steps, the wafer was heat treated in the following manner. The heat treating of the wafer had previously been found[1] to cause a migration of InP, and which resulted in a BH as illustrated in Figure I-1(c). The wafer was dipped in buffered HF for 1 min. and loaded into an LPE system with a freshly baked graphite slider, but without any growth solution. The wafer was placed in a shallow slot on the graphite slider and was covered by a graphite plate. The system was purged with H_2 and PH_3 while being heated to 670°C. The H_2- and PH_3-flow rates were chosen so that almost no surface changes were observed on plain InP substrates (except for regions near the edges) under the heating cycle used in the present work. The system reached 670°C in approximately 30 min. and stayed at that temperature for another 30 min. before being rapidly cooled.

Figure I-2(a) and (b) shows scanning electron microscope (SEM) photographs of cleaved and stained cross sections of two different wafers, one before and the other after being heat treated in the LPE system. In (a) the undercut in the quaternary etching was 2.2 μm from each side, leaving a neck-shaped quaternary region of 1.0-μm width. In some wafers, GaInAsP strips as narrow as 0.3 μm were obtained. A comparison of (a) and (b) shows that the heat treatment resulted in a marked change in the mesa shape. The corners were eroded, while the narrow undercut channels were filled in with InP. This phenomenon, apparently a transport of InP, has been reproducibly observed in 25 runs of similar experiments, with the notable exception of one in which the

1

(a) DOUBLE HETEROSTRUCTURE LASER WAFER

OXIDE MASK

InP:Zn CAP LAYER
$p \cong 5 \times 10^{17}$ cm^{-3}

GaInAsP ACTIVE LAYER
$n \cong 1 \times 10^{17}$ cm^{-3}

InP:Sn BUFFER LAYER
$n \cong 2 \times 10^{18}$ cm^{-3}

InP:Sn SUBSTRATE
$n \cong 1 \times 10^{18}$ cm^{-3}

3 μm

0.2 μm

4 μm

(b) SELECTIVE CHEMICAL ETCHING

(c) VAPOR-PHASE TRANSPORT OF InP
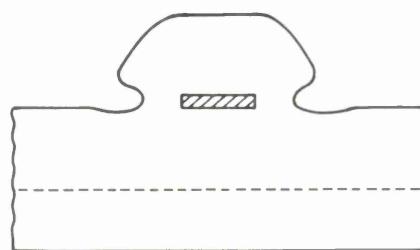
94189-1

Figure I-1.   Schematic pictures showing mesa etching and mass-transport phenomenon which result in BH. Transport of InP has been observed after heat treatment at 670° C in H₂ and PH₃ atmosphere.

2

(a)

(b)
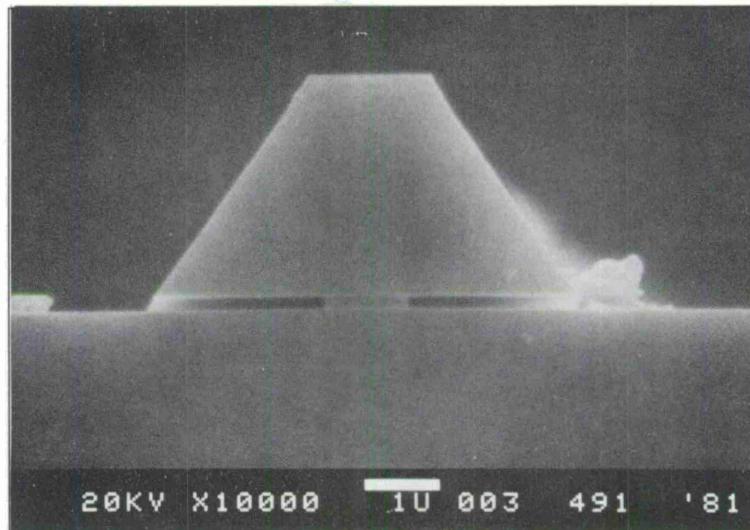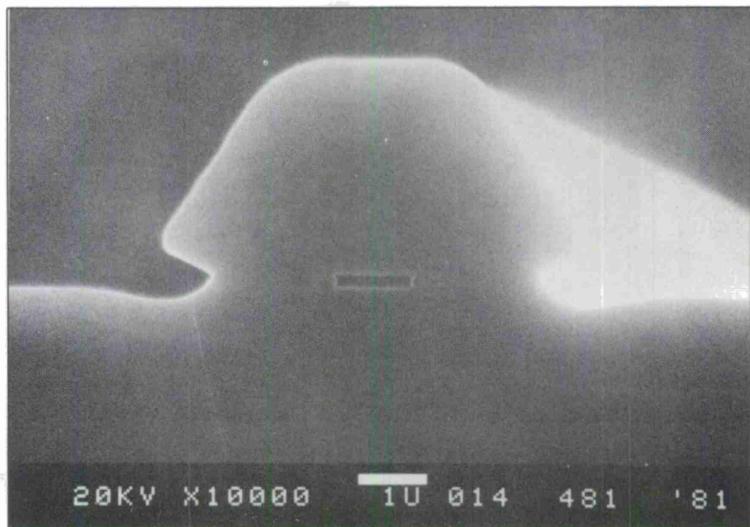
Figure I-2.   SEM micrographs showing chemically etched mesas (a) before and (b) after transport of InP. Mesa in (a) is from a bar cleaved off Wafer 491, which had a narrow (1.6 μm) mesa top, while that in (b) is from Wafer 481, for which the mesa top was wider (2.8 μm). (See Table I-1.) These cleaved facets have been stained [more heavily in (b)] in order to bring out contrast between GaInAsP and InP.

PH$_3$ flow was not used. The transported InP was generally symmetrical on the two sides of a mesa and was uniform for different mesas on the same wafer. The width of the InP varied between 0.5 and 2.0 μm, depending mainly on the amount of undercut. The recess at the base of the final mesa evident in Figure I-2(b) was reduced (or totally eliminated) with a smaller initial undercut. Mesa tops which were initially narrower than roughly 2 μm were completely rounded after the heat treatment, whereas those which were wider retained a flat top as in Figure I-2(b).

The resulting structure, which consists of a GaInAsP strip completely surrounded by InP, is ideally suited for the fabrication of a BH laser. To complete the processing, the wafer was first coated with oxide and patterned with openings on the mesa tops. After a zinc-skin diffusion through the openings in the oxide, Au-Zn alloyed contacts were made to the p$^+$-InP. The wafer was then lapped from the substrate side to a thickness of 100 μm, after which an Au-Sn alloyed contact was applied. Next, Ti (200 Å) and Au (500 Å) layers were sputter-deposited over the entire wafer on the mesa side to facilitate contacting. Individual BH lasers were then obtained by cleaving and saw-cutting.

Six wafers have been processed for BH lasers. The active region widths of each wafer shown in Table I-1 were obtained by measurements of mesas on a bar cleaved from one edge of that wafer. The BH lasers were tested in room-temperature pulsed operation with the lowest threshold currents shown in Table I-1. The yields of low-threshold devices in the first five wafers were only modest. A marked improvement was observed in the sixth wafer in which approximately 60 percent of the devices showed normal I-V characteristics and very consistent threshold currents (17 to 19 mA). This improvement was related to a special mesa structure used in this particular wafer: most areas of the wafer were protected by oxide-masks during the selective chemical etching except for stripe regions of 10-μm width on the two sides of each laser mesa. These unetched areas are expected to provide better support and protection for the laser mesas.

TABLE I-1			
Some Properties of the GaInAsP/InP BH Lasers Fabricated by the Transport of InP			
Wafer	Active Region Widths (μm)	Lowest Threshold Current (mA)	Device Length (μm)
475	3.9 to 4.5	33.0	406
476	1.8 to 2.5	20.0	254
481	0.7 to 1.4	13.8	305
489	0.7 to 1.5	9.0	279
491	1.0 to 2.2	58.0	254
513	3.0 to 3.6	17.0	279

4

The lowest threshold current obtained to date was 9.0 mA. Further reduction could well be achieved by using shorter devices and narrower active regions. Nevertheless, the present low thresholds are already comparable to or better than those obtained by more conventional fabrication techniques,[2-15] for which the lowest reported value was 10 mA (Reference 15). It is important to note that the new technique described here is considerably simpler than those reported previously, since it eliminates the need for the LPE regrowth of burying layers. The latter not only requires all the special precautions for LPE regrowth, but also demands critical control of layer thicknesses in order to reduce leakage current. In the present structure, the burying sidewalls of transported InP are just wide enough to provide mode confinement, but narrow enough to minimize current leakage. Moreover, the InP transport has been found to be very reproducible and easily controlled.

With respect to the transport of InP, the driving force for the phenomenon is probably a surface-energy minimization. It is also likely that the presence of the PH_3 plays an important role in the transport process. However, detailed study of the transport kinetics has not yet been attempted. The experimental parameters used in the present work were those for which the process was first observed. To our knowledge, this is a novel phenomenon and may find other applications in device fabrication.

<div align="right">

Z.L. Liau
J.N. Walpole

</div>
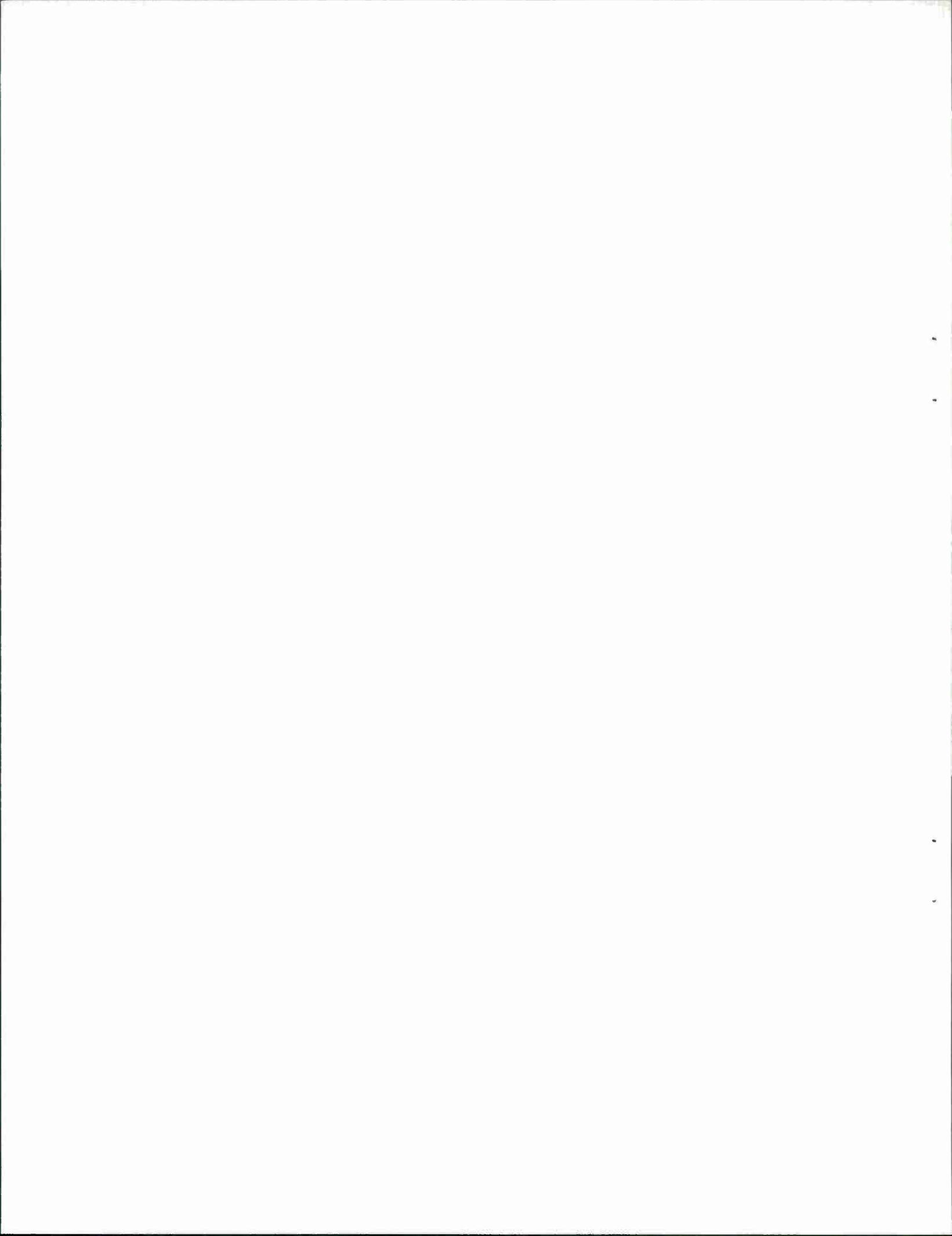
II. A SLOW SELECTIVE ETCH FOR GaInAsP GROWN ON InP

The technology for fabricating laser diodes, detectors, and optical waveguides in GaInAsP/InP epitaxial wafers requires the use of suitable etching techniques for providing smooth, damage-free surfaces, precise pattern geometries, and preferential and reproducible removal of specific layers. Several previous publications have reported slow, controllable etches for InP (References 16 through 20) and etches for selectively removing InP layers grown over GaInAsP (Reference 21). Little has been reported on slow etches for GaInAsP or on selectively etching GaInAsP on InP. Here we describe etch rate and surface morphology results obtained using a dilute sulfuric acid, hydrogen peroxide, and water etch, which has proven to be a slow selective etch for GaInAsP.

The samples used in these experiments were (100) LPE-grown GaInAsP/InP heterojunction wafers in which the quaternary compositions were either $Ga_{0.27}In_{0.73}As_{0.63}P_{0.37}$ [having a band-gap of 0.95 eV (λ = 1.3 μm)] or $Ga_{0.10}In_{0.90}As_{0.04}P_{0.96}$ [having a bandgap of 1.24 eV (λ = 1 μm)]. Each etch solution used was placed in a clean 200-ml pyrex beaker. The beaker was modified so that a microscope slide could be mounted inside. The solution was stirred continuously by means of a Teflon-coated magnetic stirrer. Part of each sample to be etched was masked with SiO_2 so that etch depth could be measured. For etching, the sample was mounted on a microscope slide using apiezon wax. After etching, the mask was removed. The sample was rinsed, dried, and inspected. The etch depth was measured with a Dek-tak surface profiler.

Slow controllable etches suitable for removing thin layers of InP are generally not usable with GaInAsP. For example, we have found that iodic acid etches[17] GaInAsP in a nonuniform manner, leaving very badly pitted surfaces. Potassium-ferrocyanide potassium-hydroxide solutions, which are often used to delineate p-n junctions in the III-V compounds, etch GaInAsP faster than InP and have been used as a selective etch.[18] The selectivity, however, depends on the doping of the InP as well as the composition of the etch solution.

Sulfuric acid-peroxide-based etches, which are commonly used as fast-polishing etches for GaAs, etch InP slowly.[22] For example, we have found that a 3 H_2SO_4:1 H_2O_2:1 H_2O solution at room temperature etches InP at about 200 Å/min. By decreasing the volume of H_2SO_4 and increasing the volume of water, the etch rate in InP can be reduced to a negligible value while maintaining a reasonable etch rate for most GaInAsP lattice-matched compositions, except those very close to InP. As shown in Figure II-1, a 1 H_2SO_4:1 H_2O_2:10 H_2O room-temperature solution etches (100) $Ga_{0.27}In_{0.73}As_{0.63}P_{0.37}$ (λ_g = 1.3 mm) at a very constant etch rate of 1000 Å/min. The etched GaInAsP surface appeared to be free of any etch-related defects. Figure II-2 shows a photomicrograph of a double heterojunction wafer in which the top InP layer was removed from most of the wafer using concentrated HCl (a selective etch for InP). Different areas of the GaInAsP layer were then etched for different times using 1 H_2SO_4: 1 H_2O_2:10 H_2O. The etched surfaces have the same surface texture as the originally exposed quaternary surface. For (100) $Ga_{0.10}In_{0.90}As_{0.04}P_{0.96}$ (λ_g = 1.04 μm), the etch rate (see Figure II-1) drops to about 75 Å/min. The etch depth on (100) InP could not be measured after an hour's etch time although a fine
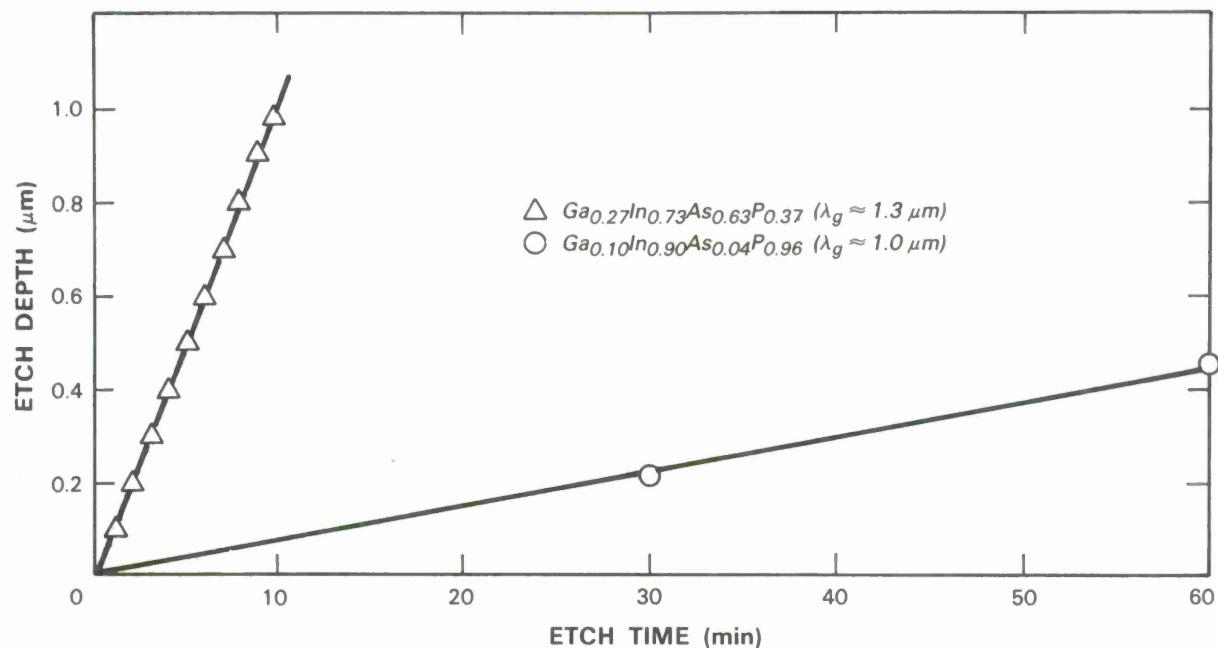
Figure II-1.   Etch depth vs etch time obtained on a $Ga_{0.27}In_{0.73}As_{0.63}P_{0.37}$ and a $Ga_{0.10}In_{0.90}As_{0.04}P_{0.96}$ layer etched in a room-temperature 1 H_2SO_4:1 H_2O_2:10 H_2O solution.
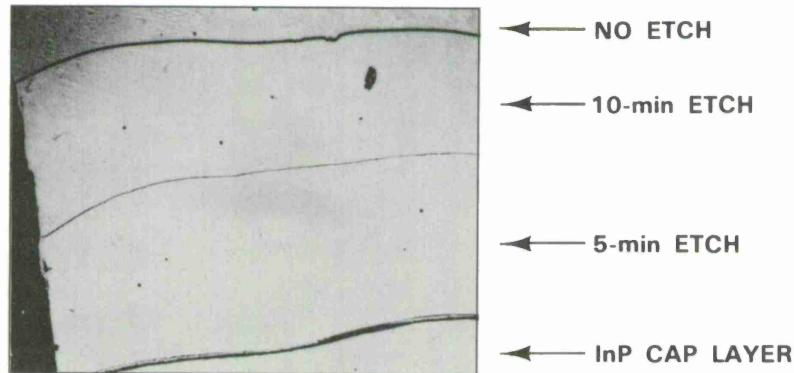
Figure II-2.   Photomicrograph of a $Ga_{0.27}In_{0.73}As_{0.63}P_{0.37}$/InP double heterojunction wafer in which most of top InP was removed in concentrated HCl and different areas of quaternary layer etched for times indicated (no etch, 5-min etch, and 10-min etch) in a 1 H_2SO_4:1 H_2O_2:10 H_2O solution.

8

demarcation line between the etched and unetched areas of the samples was observed. The surface quality of the InP exposed to the dilute sulfuric acid etch was good (see InP surface in Figure II-2, which was exposed to the dilute sulfuric acid etch). The same result was obtained on (100)-oriented liquid encapsulated Czochralski (LEC) InP samples doped with either Zn and Sn to concentrations greater than 10^{18} cm^{-3}. Various dilutions of H_2SO_4:H_2O_2:H_2O should prove useful as slow selective etches for GaInAsP in a variety of applications.

G.A. Ferrante
J.P. Donnelly
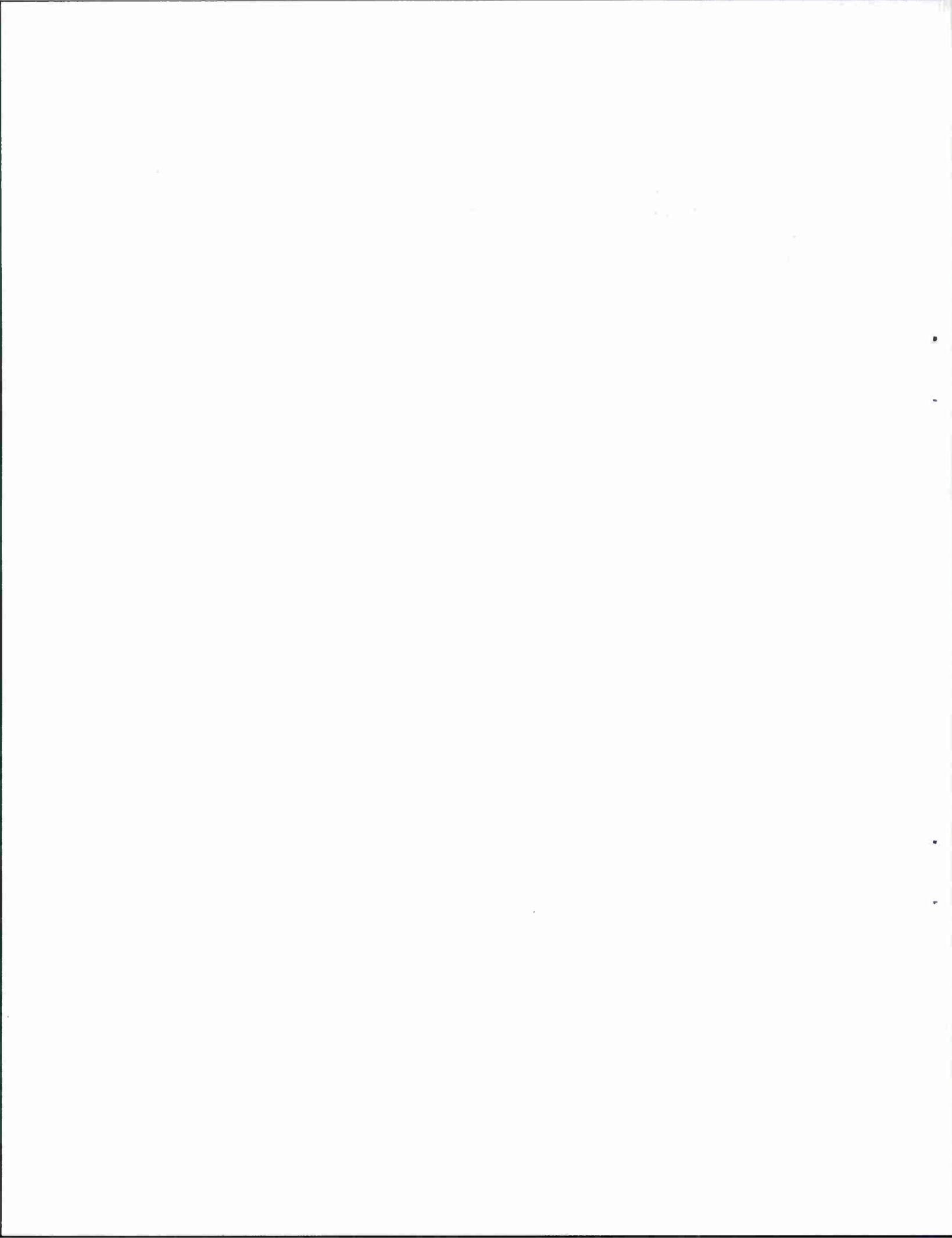
III. THREE-GUIDE OPTICAL COUPLERS IN GaAs

Optical couplers are an important component of almost all integrated optical circuit concepts. There have been a number of reports on two-guide optical couplers including experimental results on couplers fabricated on GaAs (References 23 through 31), InP (Reference 32), and GaInAsP (Reference 33). Work reported to date on three-guide couplers has been theoretical.[34,35] When used to couple power from one outside guide to the other outside guide, the three-guide coupler has sharper transfer characteristics than a similar two-guide coupler. It has been proposed to use this feature for improved sampling and filtering.[35] Another possible application of three-guide couplers is their use as symmetrical power dividers and combiners.

The symmetrical three-guide couplers used in these experiments are composed of three slab-coupled rib-waveguides in close proximity as shown in Figure III-1(a). The individual waveguides were designed to be single mode[36] and consist of a rib etched in a nominally undoped n^--GaAs epitaxial layer grown on a (100)-oriented 2×10^{18} cm^{-3} n^+-GaAs substrate. The epitaxial layer was n-type with a carrier concentration of 1×10^{15} cm^{-3} and had a thickness of 4.2 μm. Details of the fabrication can be found in Reference 37. Note that, because of an orientation-dependent etch rate, the ribs in Figure III-1(a) are actually trapezoidal in shape. The mean width of a rib is 4.75 μm, and the mean spacing or separation between ribs is 4.25 μm. The height of the rib is 1.5 μm. After the ends were cleaved, the sample was mounted on a high-performance translation-rotary stage for optical evaluation. Following evaluation at one length, the sample was cleaved to a shorter length and the evaluation repeated.

Optical measurements were made using an end-fired coupling scheme.[26] Radiation from a single-mode CW GaInAsP/InP double-heterojunction laser operating at 1.28 μm was collimated, passed through a polarizer, aperture and neutral density filter, and focused on the cleaved input face of the waveguide sample using a microscope objective. The electric field of the input light was polarized parallel to the plane of the slab. The input from the waveguide sample was focused by a beam-splitting microscope into two images. One output image went to an infrared TV camera system; the other image was passed through a pinhole aperture onto a Ge photodiode. The output image could either be scanned across the pinhole aperture using a scanning mirror, or the aperture could be precisely translated across the image. When the scanning mirror was used, the output of the Ge detector could be displayed on an oscilloscope as a function of effective position. For comparison purposes, single isolated guides, three- and two-guide couplers were evaluated.

Since an exact analysis of these three-guide couplers is not possible, an extension of the effective index method[38,39] was used to obtain an approximate analytic solution and some insight into device behavior. Details of this analysis can be found in Reference 38. In the limit of loose coupling between guides,[34,35] power input into the center guide will be symmetrically transferred to the two outside guides in a coupling length, $L_{CT \to 0}$. This coupling length is $\sqrt{2}$ times larger than that of a similar two-guide coupler. For power into an outside guide of the three-guide coupler, all the power is transferred to the other outside guide in a distance $L_{01 \to 02}$, which is

11
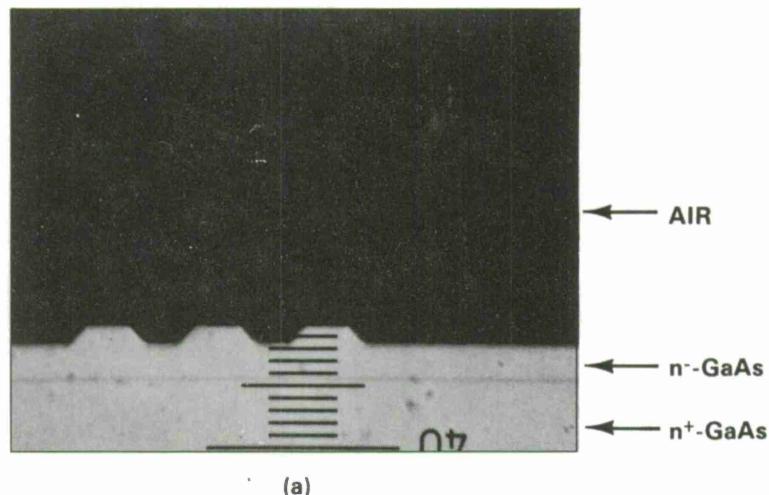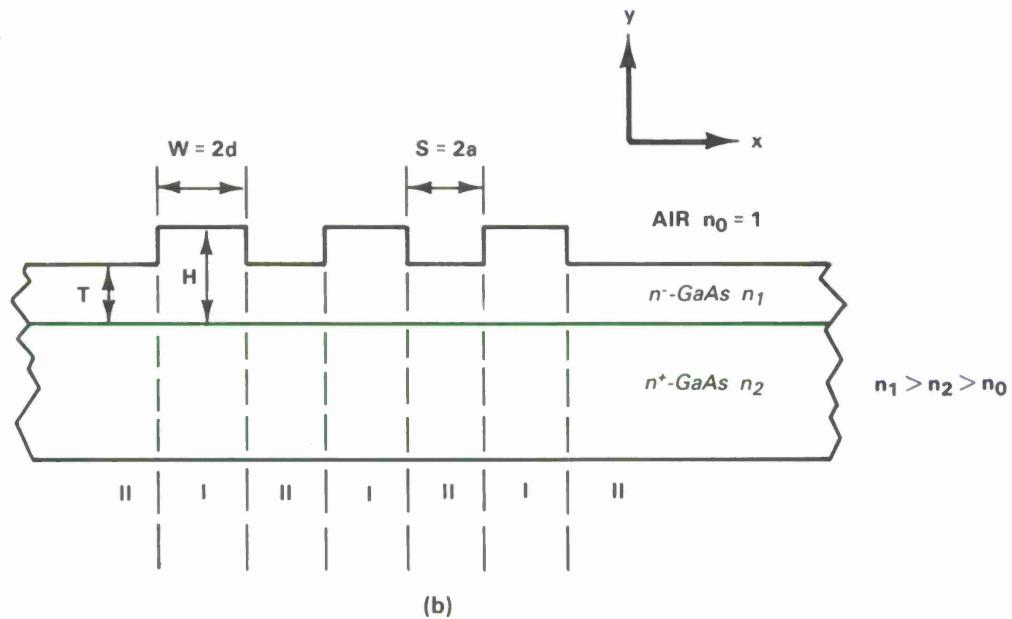
Figure III-1.   (a) Photomicrograph of cleaved cross section of GaAs three-guide coupler. Sample has been treated with a stain/etchant to reveal n^- - n^+ interface. Scale on photomicrograph is 1 µm/div. (b) Schematic cross section of three-guide coupler with rectangular ribs of a width equal to average width (same cross-sectional area) of actual guides. Regions I and II are modeled as slab waveguides to determine effective guide index in different portions on n^--layer.

twice as long as that needed to symmetrically couple power from the center guide to the two out-side guides.

For the isolated single guides, a single intensity maximum was observed under the rib as expected. The outputs of the two- and three-guide couplers, as a function of length, were in good agreement with the output expected from theory.

The best fit to the experimental data gave a coupling length for symmetrically transferring power from the center guide of a three-guide coupler to the two outside guides, $L_{CT \to 0}$, of ≈ 3.2 mm. Figure III-2(a) shows the relative power out of each guide of a three-guide coupler vs length for power input into the center guide. Figure III-2(b) is an oscilloscope and TV output obtained for a length of 3.2 mm. Most of the asymmetry in the oscilloscope photograph is due to the scanning optics. The solid curves in Figure III-2(a) are plots of the results expected from loose-coupling theory using a coupling length of 3.2 mm. The relative power output of all three guides is a reasonably good fit to the approximate power-division equations. At a length of 3.2 mm, the power input to the center guide is divided between the two outside guides, with min-imal ($\leqslant 1$ percent) remaining in the center guide.

With the effective guide index method, the coupling length to transfer power from the center guide to the two outside guides ($L_{CT \to 0}$) was calculated to be 2.85 mm using the loose-coupling approximation, and 2.79 mm using the actual eigenmode equations to calculate the propagation constants of the modes of the three-guide coupler. In these calculations, the average width of the trapezoidal ribs (4.75 μm) and average spacing (4.25 μm) were used.[36] The effective index of the epitaxial layer n_1 was taken[40] as 3.43, and the usual free carrier effect on index was used to determine the index of the n^+-substrate n_2. The agreement between the calculated and experimen-tal coupling lengths is quite good (≈ 12.5-percent difference). It is not clear how much of the dif-ference is due to inherent limitations in the effective guide index calculation and how much is due to the use of inaccurate waveguide parameters.

Figure III-3(a) shows the relative power out of each guide of the same three-guide coupler vs length for power into an outside guide. The oscilloscope and TV outputs at a length of 6.5 mm are shown in Figure III-3(b). The solid lines in Figure III-3(a) are plots of the results expected from loose-coupling theory with a coupling length ($L_{01 \to 02}$) twice as long as that used in Fig-ure III-2. The coupling length in the loose-coupling approximation for complete power transfer from one outside guide to the other should be 6.4 mm. The data obtained at a length of 6.5 mm, which is slightly longer, show most of the power in the coupled outside guide (≈ 86 percent), a small amount in the center guide (≈ 11.5 percent), and only ≈ 2.5 percent in the input outside guide. Since in this case there are three modes whose phase velocities are not related to each other in a simple way (only an approximation for loose coupling), the beats between these modes and therefore the power transfer are not expected to be as good as in the case where the power input was into the center guides. Although it is not clear why there is so much residual power in the center guide at a length of 6.5 mm, there is fairly good overall agreement between the mea-sured relative powers and those expected from the coupling theory.

CENTER

COUPLED

RELATIVE OUTPUT

1 0

0 5

0   2   4   6   8   10

LENGTH (mm)

(a)

FOR 3.2-mm LENGTH:

POWER
IN

COUPLED   COUPLED

CENTER

20mV   >200µS

COUPLED   COUPLED

CENTER

COUPLED   COUPLED

CENTER

(b)

94189-6
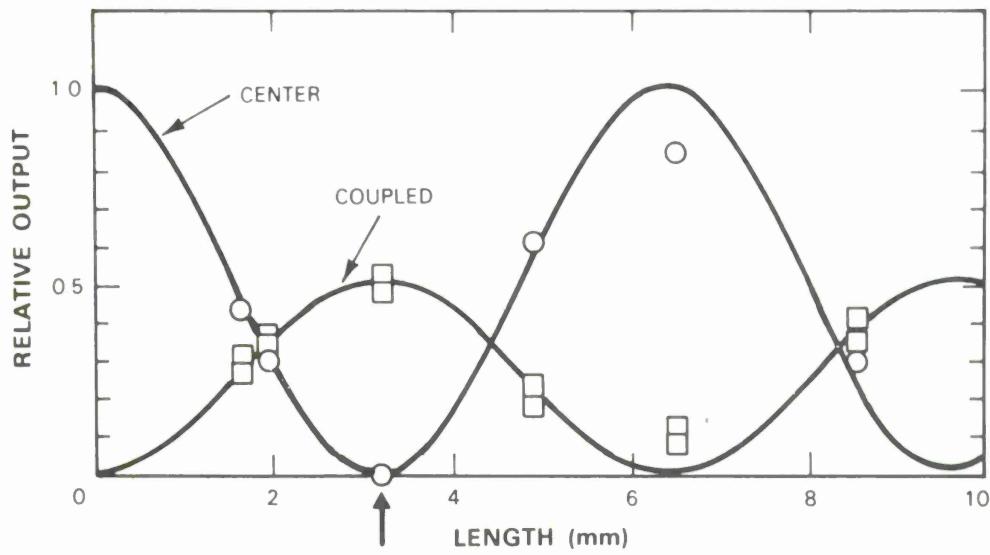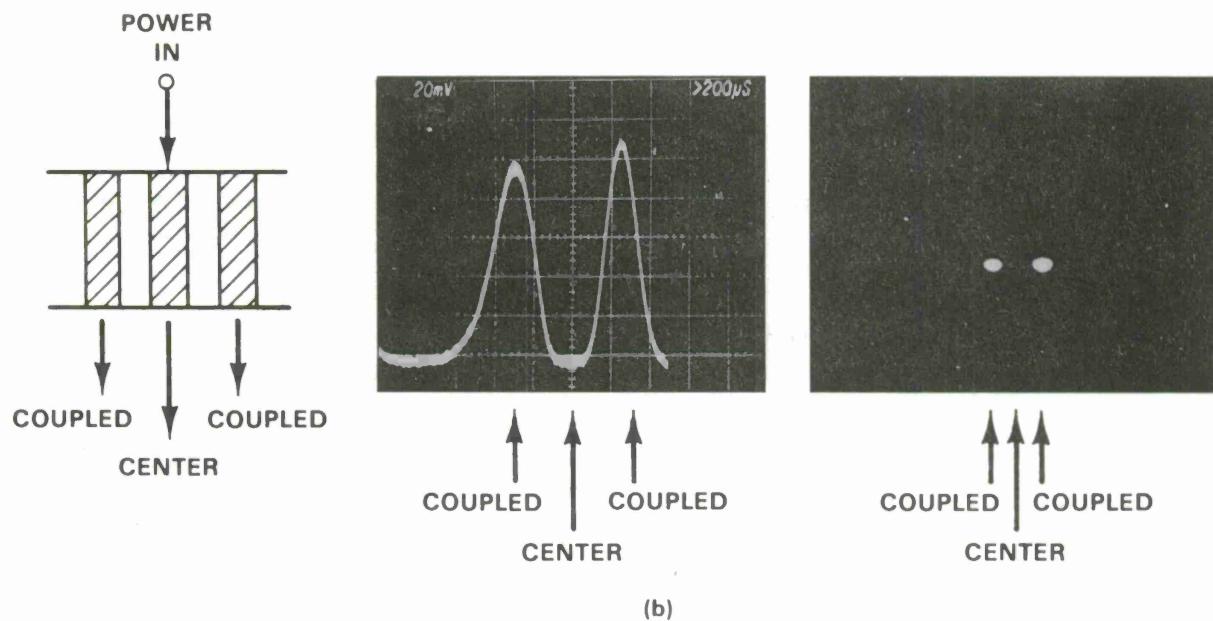
Figure III-2. (a) Relative output power out of each guide as a function of length for a three-guide coupler with input power into center guide. b) Outputs obtained on oscilloscope and TV monitor for a length of 3.2 mm.

14
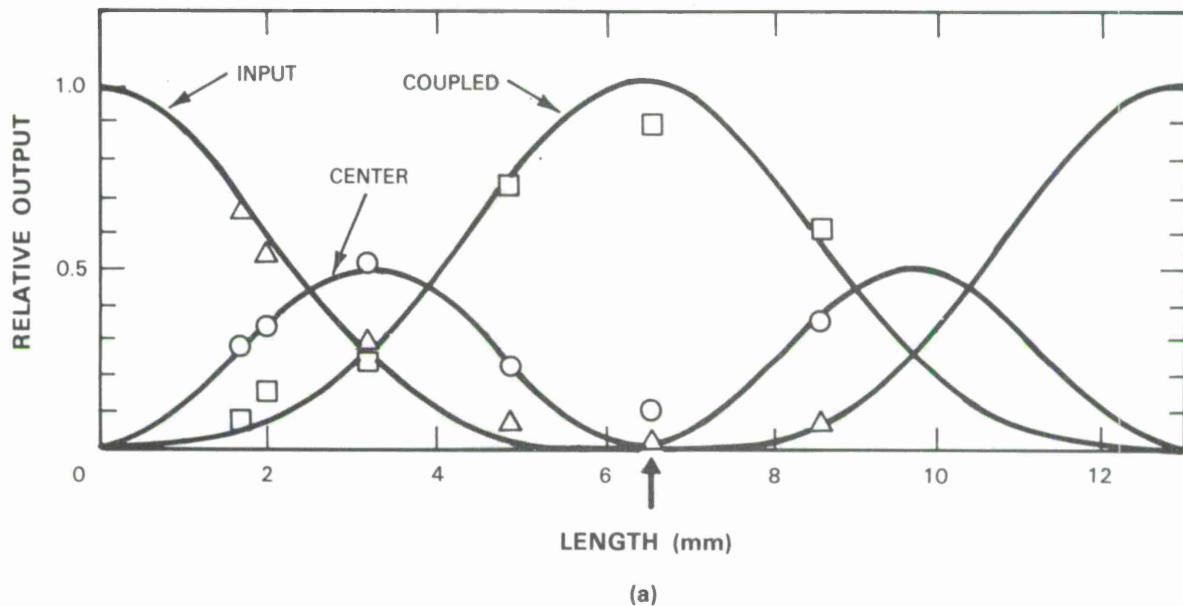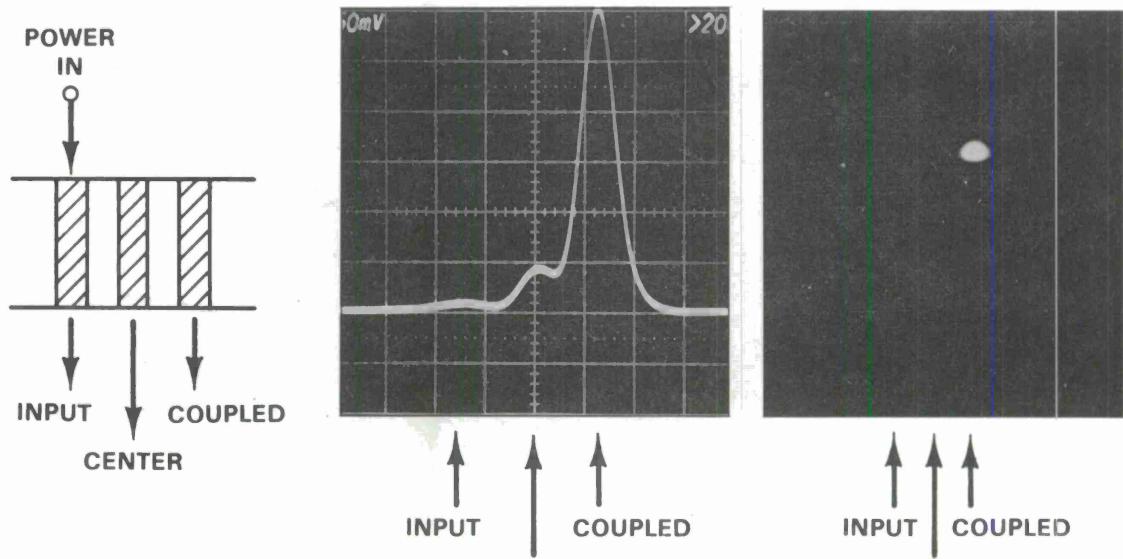
Figure III-3. (a) Relative output power of each guide as a function of length for a three-guide coupler with input power into one of outside guides. (b) Outputs obtained on oscilloscope and TV monitor for a length of 6.5 mm.

15
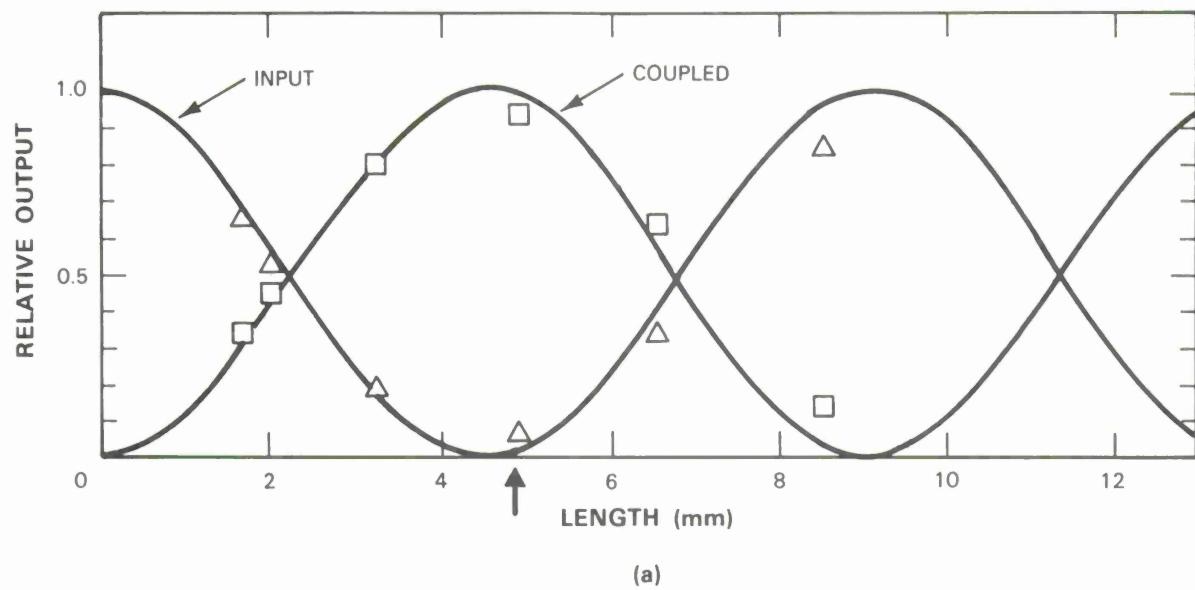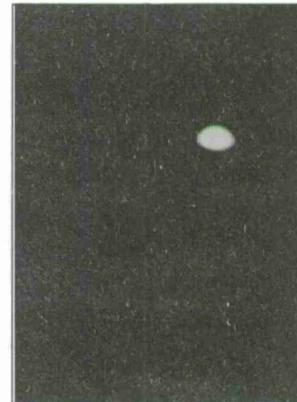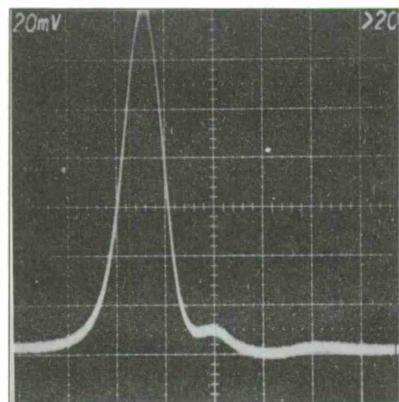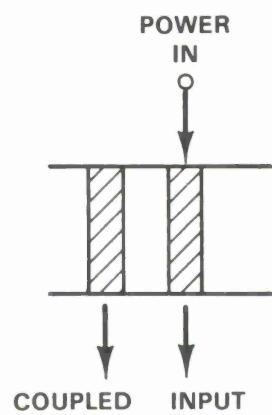
Figure III-4. (a) Relative output power of each guide as a function of length for at two-guide coupler. (b) Outputs obtained on oscilloscope and TV monitor for a length of 4.9 mm.

16

For comparison, Figure III-4(a) shows the relative output of each guide of a two-guide coupler vs length, and Figure III-4(b) shows the oscilloscope and TV outputs at a length of 4.9 mm. The solid line represents the power-division equations of a two-guide coupler with a coupling length $\sqrt{2}$ times larger than that of a three-guide coupler with power input into the center guide. At a length of 4.9 mm, which is somewhat longer than the 4.5-mm coupling length, there is still almost complete power transfer from one guide to another.

In summary, symmetrical three-guide couplers, whose behavior closely approximates that predicted using an effective-index analytical method, have been fabricated in GaAs.

<div align="right">

J.P. Donnelly
N.L. DeMeo
G.A. Ferrante

</div>
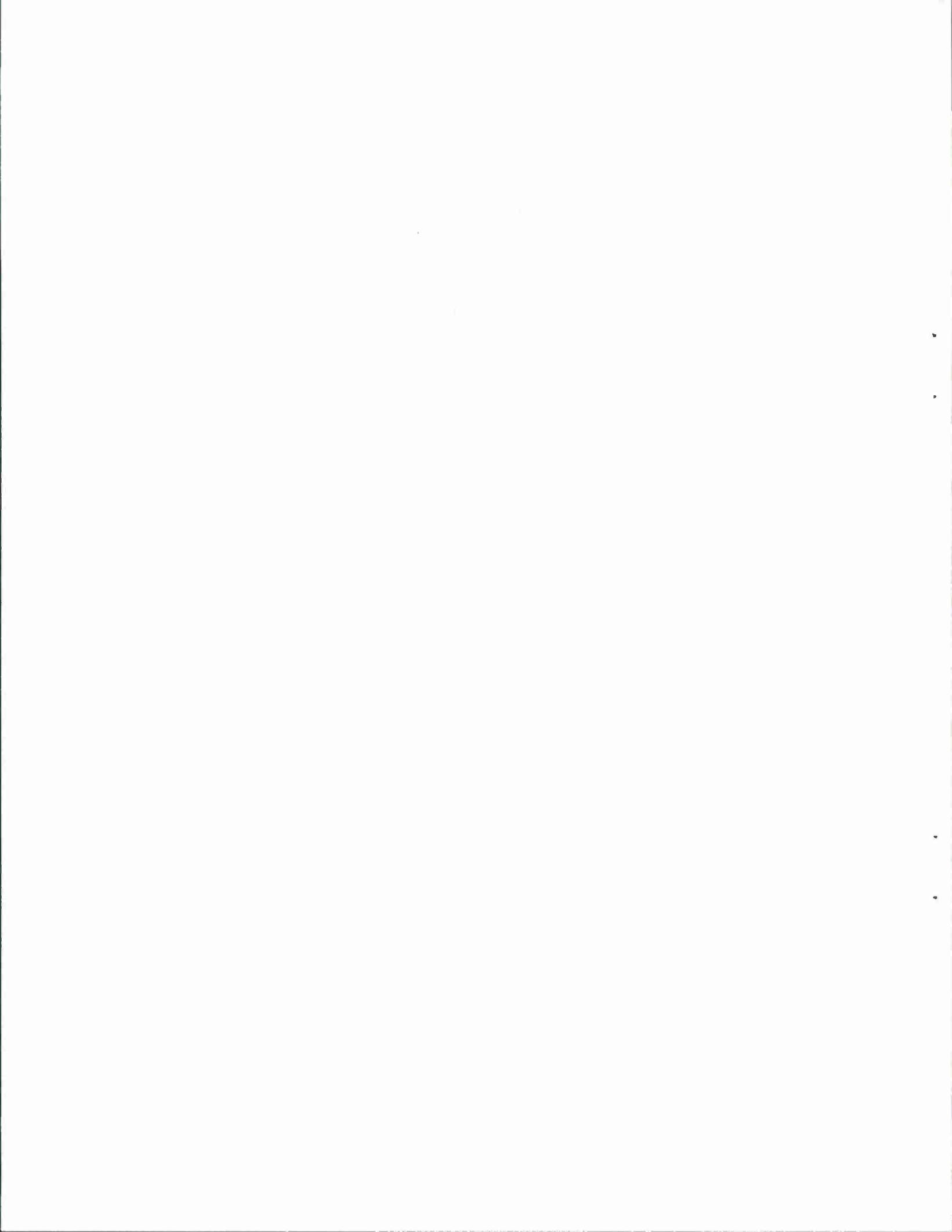
IV. CONTINUOUS MULTI-GIGAHERTZ MODULATION
OF Q-SWITCHED GaInAsP DIODE LASERS

Diode lasers capable of producing short optical pulses at high rates are being developed for applications in communications and optical signal processing. Previously we have reported the pulsed operation of an intracavity-loss modulated laser with a zinc-diffused stripe geometry amplifier section.[41,42]

We report here a CW diode laser with two electrically isolated buried-heterostructure sections that has been operated with full on/off modulation at 3 GHz. The device operation is based on a combination of gain switching and Q-switching in which both gain and loss are actively varied in a modulator section while an amplifier section is driven with a constant dc current.

The device, shown in Figure IV-1, is fabricated from a double-heterostructure wafer consisting of a p-InP cap layer, a nominally undoped GaInAsP active region, and an n$^+$-InP buffer layer on an n$^+$-InP substrate. The buried active region is formed by an etching and mass transport process.[18] The wafer is proton bombarded to produce a laser with a long amplifier section ($\approx$200 μm) and a short modulator section ($\approx$50 to 100 μm) electrically isolated by the high-resistivity bombarded region (20 μm).
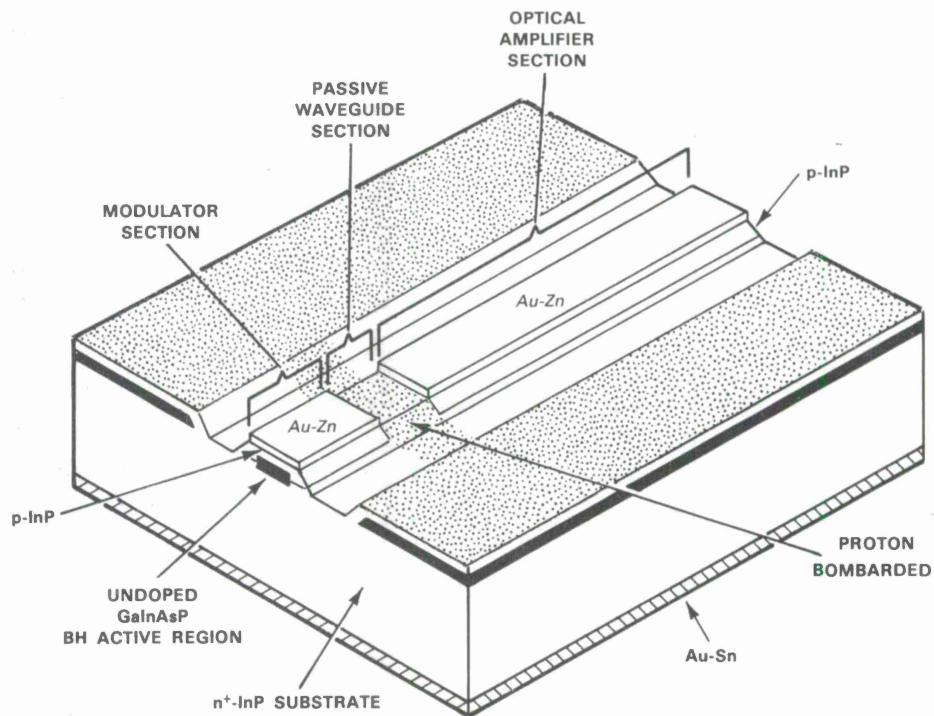
Figure IV-1.   Schematic cross section of a Q-switched diode laser. The proton bombarded region extends below the active region to isolate the amplifier and the modulator.

19

|←— 333 ps —→|
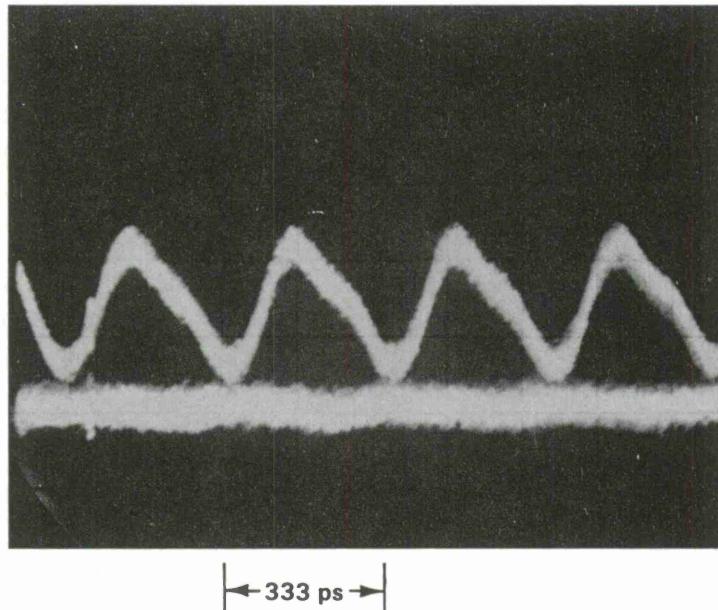
Figure IV-2.   Detected output from a Q-switched diode laser with a proton-isolated modulator at 3 GHz. About 10 mW of microwave power is required for full off/on modulation.

With uniform dc current density applied to each section, the laser threshold is as low as 17 mA. With a small forward voltage <0.8 V in the modulator, such that no significant current injection occurs, the laser threshold for current through the amplifier is over 60 mA, three times that of the uniformly pumped laser.

Full on/off modulation up to 3 GHz has been seen at a forward bias of 0.8 V with only about 10 mW of microwave power applied to the modulator and about 60 mA of dc current applied to the amplifier (Figure IV-2). As the amplifier current was increased, subharmonic operation was seen at 1.5 GHz. A substantial increase in the peak signal level was noted at the subharmonic, an indication of energy storage and Q-switching.

Under modulation, significant forward current is injected into the modulator section to switch the modulator loss rapidly into gain. A Q-switched pulse can then rapidly build and dump the electron population in both sections. Since the turn-on time of the modulator is limited only by its capacitance and the drive current, while the turn-off time is dependent on the stimulated lifetime, operation well above a gigahertz is possible, depending on how hard the sections are driven. These low-threshold lasers are capable of producing short pulses at high rates with low microwave power requirements.

D.Z. Tsang
J.N. Walpole
Z.L. Liau

20

REFERENCES

1. Z.L. Liau and J.N. Walpole, Paper WB3, Technical Digest, Topical Meeting on Integrated and Guided-Wave Optics, Optical Society of America, 1982; Solid State Research Report, Lincoln Laboratory, MIT (1981:3), p. 7, DTIC AD-A112696.

2. J.J. Hsieh and C.C. Shen, Appl. Phys. Lett. **30**, 429 (1977), DDC AD-A063419.

3. M. Hirao, A. Doi, S. Tsuji, M. Nakamura, and K. Aiki, J. Appl. Phys. **51**, 4539 (1980).

4. Y. Itaya, T. Tanbun-Ek, K. Kishino, S. Arai, and Y. Suematsu, Jpn. J. Appl. Phys. **19**, L141 (1980).

5. H. Nagai, Y. Noguchi, K. Takahei, Y. Toyoshima, and G. Iwane, Jpn. J. Appl. Phys. **19**., L218 (1980).

6. T. Murotani, E. Oomura, H. Higuchi, H. Namizaki, and W. Susaki, Electron. Lett. **16**, 566 (1980).

7. R.J. Nelson, R.B. Wilson, P.D. Wright, P.A. Barnes, and N.K. Dutta, IEEE J. Quantum Electron. **QE-17**, 202 (1981).

8. S. Arai, M. Asada, T. Tanbun-Ek, Y. Suematsu, Y. Itaya, and K. Kishino, IEEE J. Quantum Electron. **QE-17**, 64 (1981).

9. E. Oomura, T. Murotani, H. Higuchi, H. Namizaki, and W. Susaki, IEEE J. Quantum Electron. **QE-17**, 646 (1981).

10. P.C. Chen, K.L. Yu, S. Margalit, and A. Yariv, Appl. Phys. Lett. **38**, 301 (1981).

11. W. Ng, C.S. Hong, H. Manasevit, and P.D. Dapkus, Appl. Phys. Lett. **39**, 188 (1981).

12. W. Ng, C.S. Hong, H. Manasevit, and P.D. Dapkus, Third International Conference on Integrated Optics and Optical Fiber Communication, (IOCC '81), Technical Digest, p. 52.

13. I. Mito, K. Kaede, M. Kitamura, K. Kobayashi, and S. Matsushita, Third International Conference on Integrated Optics and Optical Fiber Communication, (IOCC '81), Technical Digest, p. 44.

14. E. Oomura, H. Higuchi, R. Hirano, H. Namizaki, T. Murotani, W. Susaki, and K. Shirahata, Third International Conference on Integrated Optics and Optical Fiber Communication, (IOCC '81), Technical Digest, p. 44.

15. M. Nakamura and S. Tsuji, IEEE J. Quantum Electron. **QE-17**, 994 (1981).

16. R. Becker, Solid State Electron. **16**, 1241 (1973).

17. A.R. Clawson, D.A. Collins, D.I. Elder, and T.J. Monroe, NOSC Technical Note 592, Naval Ocean Systems Center, San Diego, California (13 December 1978).

18. Z.L. Liau and J.N. Walpole, Appl. Phys. Lett. **40**, 568 (1982).

19. S. Adachi and H. Kawaguchi, J. Electrochem. Soc. **128**, 1342 (1981).

20. S. Adachi, H. Kawaguchi, and G. Iwane, J. Mater. Sci. **16**, 2449 (1981).

21. S.B. Phatak and G. Kelner, J. Electrochem. Soc. **126**, 287 (1979).

22. Y. Nishitani and T. Kotani, J. Electrochem. Soc. **126**, 2269 (1979).

23. S. Somekh, E. Garmire, A. Yariv, H. L. Garvin, and R. G. Hunsperger, Appl. Phys. Lett. **22**, 46 (1973).

24. S. Somekh, E. Garmire, A. Yariv, H.L. Garvin, and R.G. Hunsperger, Appl. Opt. **13**, 327 (1974).

25. J.C. Campbell, F.A. Blum, D.W. Shaw, and K.L. Lawley, Appl. Phys. Lett. **27**, 202 (1975).

26. F.J. Leonberger, J.P. Donnelly, and C.O. Bozler, Appl. Phys. Lett. **29**, 652 (1976), DDC AD-A037627.

27. F.J. Leonberger, J.P. Donnelly, and C.O. Bozler, Appl. Opt. **17**, 2250 (1978), DDC AD-A060932.

28. J.C. Shelton, F.K. Reinhart, and R.A. Logan, Appl. Opt. **17**, 2548 (1978).

29. J.C. Shelton, F.K. Reinhart, and R.A. Logan, J. Appl. Phys. **50**, 6675 (1979).

30. A. Carenco, L. Menigaux, and P.L. Delpech, J. Appl. Phys. **50**, 5139 (1979).

31. A. Carenco and L. Menigaux, J. Appl. Phys. **51**, 1325 (1980).

32. A. Carenco, N.T. Linh, and L. Menigaux, Appl. Phys. Lett. **40**, 653 (1982).

33. N.L. DeMeo, F.J. Leonberger, and S.H. Groves, Topical Meeting on Integrated and Guided-Wave Optics, Pacific Grove, California, 6-8 January 1982, Digest of Technical Papers, pp. WD7-1 - WD7-3.

34. K. Iwasaki, S. Kurazono, and K. Itakuna, Electron. Commun. Jpn. **58-C**, 100 (1975).

35. H.A. Haus and C.G. Fonstad, Jr., IEEE J. Quantum Electron. **QE-17**, 2321 (1981).

36. E.A.J. Marcatili, Bell Syst. Tech. J. **53**, 645 (1974).

37. J.P. Donnelly, N.L. DeMeo, and G.A. Ferrante, IEEE J. Lightwave Technol. **LT-1**, 417 (1983).

38. V. Ramaswamy, Bell. Syst. Tech. J. **53**, 697 (1974).

39. W.V. McLevige, T. Itoh, and R. Mittra, IEEE Trans. Microwave Theory Tech. **MTT-23**, 788 (1975).

40. D.T.F. Marple, J. Appl. Phys. **35**, 124 (1964).

41. D.Z. Tsang, J.N. Walpole, S.H. Groves, J.J. Hsieh, and J.P. Donnelly, Appl. Phys. Lett. **38**, 120 (1981), DTIC AD-A103344.

42. Solid State Research Report, Lincoln Laboratory, MIT (1981:2), pp. 1-3, DTIC AD-A110947.
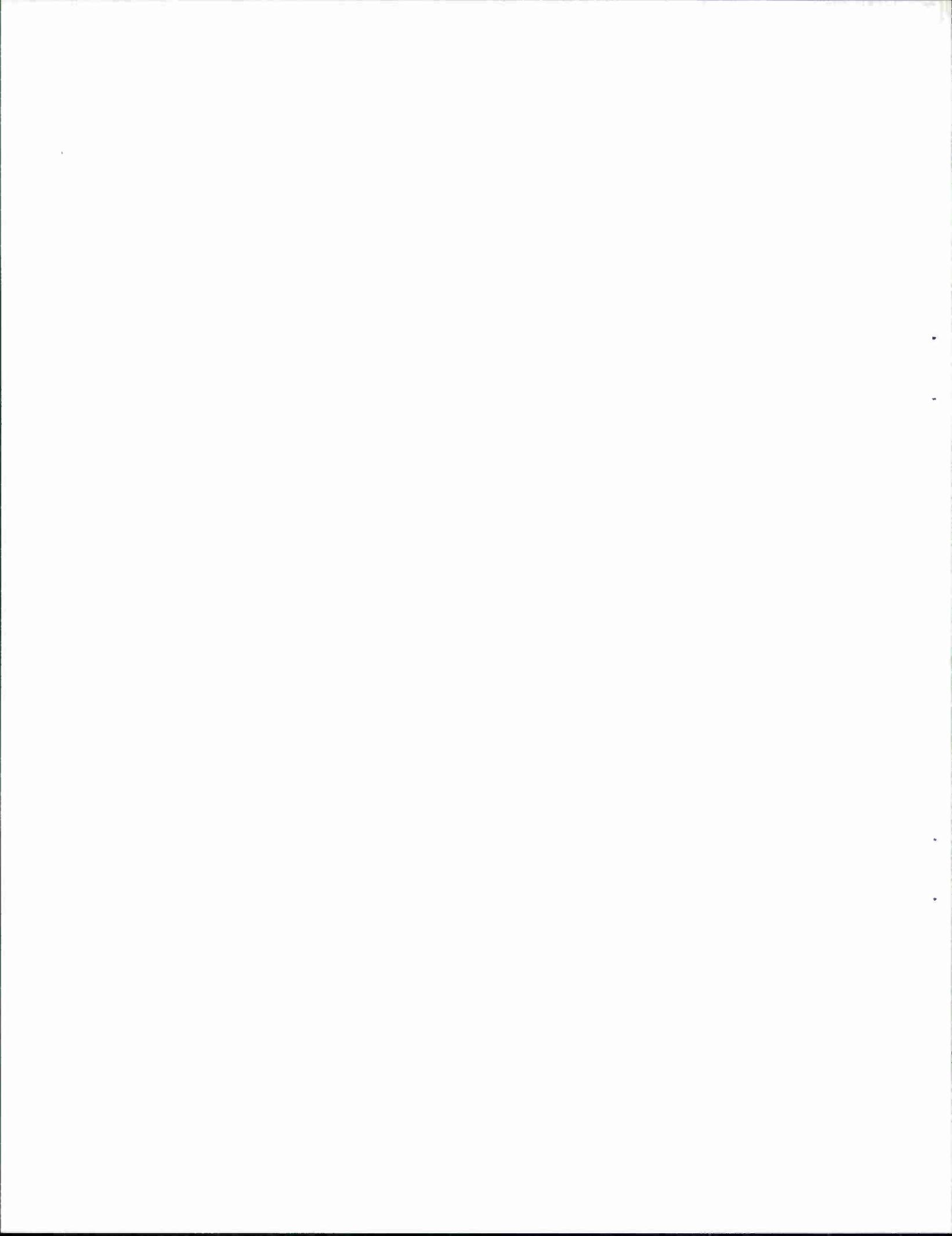
APPENDIX A
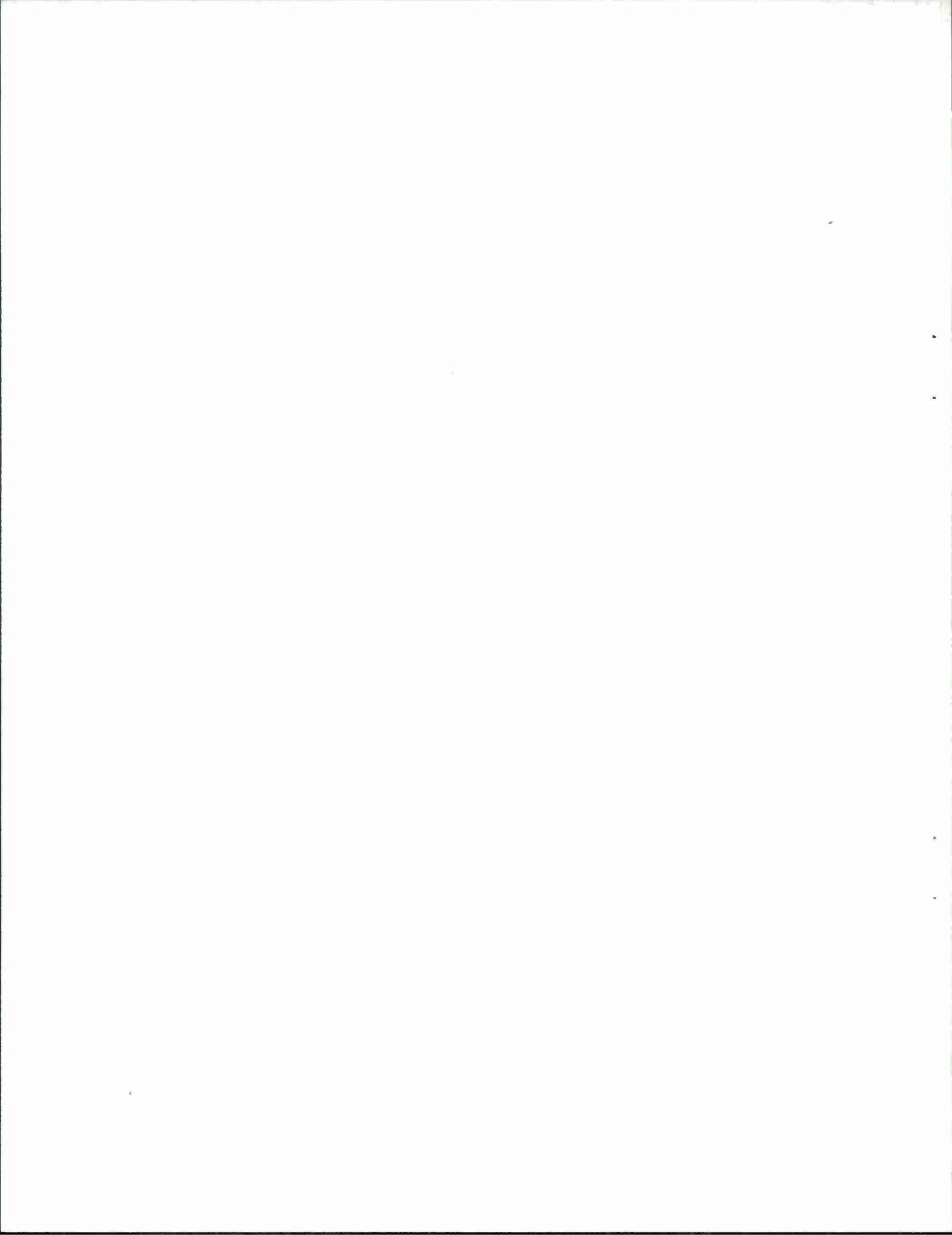
A novel technique for GaInAsP/InP buried heterostructure laser fabrication

Z. L. Liau and J. N. Walpole

Lincoln Laboratory, Massachusetts Institute of Technology, Lexington, Massachusetts 02173

A simple fabrication technique for GaInAsP/InP buried heterostructure lasers has been developed based on a newly observed mass transport phenomenon on chemically etched InP mesas. Threshold currents as low as 9.0 mA have been obtained.

PACS numbers: 42.55.Px, 73.40.Lq, 81.60.Hv

In this letter, we report the development of a novel technique for the fabrication of GaInAsP/InP buried heterostructure (BH) lasers. It is based on a mass transport phenomenon which was recently observed during the fabrication of integrated laser-waveguide structures.[1] This technique is considerably simpler and more easily controlled than previously reported ones,[2-15] and has resulted in BH lasers with threshold currents as low as 9.0 mA.

The experimental procedure is illustrated in Fig. 1. The starting wafer was a double heterostructure one, prepared by conventional liquid-phase epitaxial (LPE) techniques on a (100) InP substrate. (In separate experiments, broad area la-

(a) DOUBLE HETEROSTRUCTURE LASER WAFER
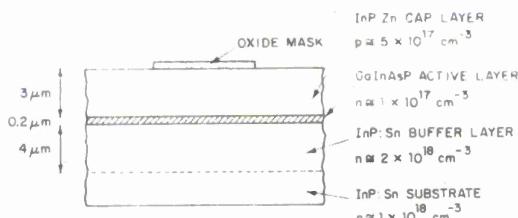
(b) SELECTIVE CHEMICAL ETCHING
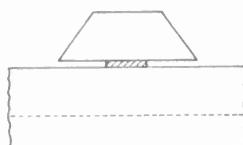
(c)   TRANSPORT OF InP
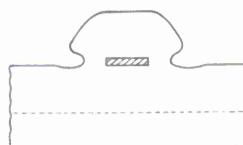
FIG. 1. Schematic pictures showing the mesa etching and the mass transport phenomenon which result in the buried heterostructure. The transport of InP has been observed after a heat treatment at 670 °C in H_2 and PH_3 atmosphere.

(a)

(b)

FIG. 2. SEM micrographs showing the chemically etched mesa (a) before and (b) after the transport of InP. The mesa in (a) is from a bar cleaved off Wafer 491, which had a narrow (1.6 μm) mesa top, while that in (b) is from Wafer 481, for which the mesa top was wider ($\sim 2.8 \mu$m) (see Table I). These cleaved facets have been stained [more heavily in (b)] in order to bring out the contrast between GaInAsP and InP.

sers fabricated from similar wafers had threshold current densities of 0.9 to 1.3 kA/cm^2.) Oxide-stripe masks 5.0–6.0 μm wide on 250-μm centers were first fabricated on the wafer, with the stripes parallel to either (011) or (01$\bar{1}$) crystallographic directions. Two steps of selective chemical etching were taken in order to produce the mesa structure shown in Fig. 1(b). First, concentrated HCl was used to remove the unprotected InP cap layer. While being etched, the wafer was well agitated and closely monitored visually for the slight color difference between the quaternary layer and the InP. The etching was immediately terminated when the InP cap layer was completely etched through. The $Ga_{0.27}In_{0.73}As_{0.63}P_{0.37}$ active layer thus exposed was then removed with a 50-ml aqueous solution of 10-g KOH and 0.2-g $K_3Fe(CN)_6$. Additional etching time, beyond that required to remove the quaternary layer, was sometimes used, depending on the desired amount of undercutting [Fig. 1(b)].

After completion of the etching steps the wafer was heat treated in the following manner which had previously been found[1] to cause a migration of InP, and which resulted in a buried heterostructure as illustrated in Fig. 1(c). The wafer was dipped in buffered HF for 1 min and loaded into an LPE system with a freshly baked graphite slider, but without any growth solution. The wafer was placed in a shallow slot on the graphite slider and was covered by a graphite plate. The system was purged with H_2 and PH_3 while being heated to 670 °C. The H_2 and PH_3 flow rates were chosen so that almost no surface changes were observed on plain InP substrates (except for regions near the edges) under the heating cycle used in the present work. The system reached 670 °C in

approximately 30 min and stayed at that temperature for another 30 min before being rapidly cooled down.

Figure 2 shows scanning electron microscope (SEM) photographs of cleaved and stained cross sections of two different wafers, one before and the other after being heat treated in the LPE system. In (a) the undercut in the quaternary etching was 2.2 μm from each side, leaving a neck-shaped quaternary region of 1.0-μm width. In some wafers GaInAsP strips as narrow as 0.3 μm were obtained. A comparison of (a) and (b) shows that the heat treatment resulted in a marked change in the mesa shape. The corners were eroded, while the narrow undercut channels were filled in with InP. This phenomenon, apparently a transport of InP, has been reproducibly observed in 25 runs of similar experiments, with the notable exception of one in which the PH_3 flow was not used. The transported InP was generally symmetrical on the two sides of a mesa and was uniform for different mesas on the same wafer. The width of the InP varied between 0.5 and 2.0 μm, depending mainly on the amount of undercut. The recess at the base of the final mesa evident in Fig. 2(b) was reduced (or totally eliminated) with a

28

TABLE I. Some properties of the GaInAsP/InP BH lasers fabricated by the transport of InP.

Wafer	Active region widths (μm)	Lowest threshold current (mA)	Device length (μm)
475	3.9–4.5	33.0	406
476	1.8–2.5	20.0	254
481	0.7–1.4	13.8	305
489	0.7–1.5	9.0	279
491	1.0–2.2	58.0	254

smaller initial undercut. Mesa tops which were initially narrower than roughly $2\,\mu$m were completely rounded after the heat treatment, whereas those which were wider retained a flat top as in Fig. 2(b).

The resulting structure, which consists of a GaInAsP strip completely surrounded by InP, is ideally suited for the fabrication of a buried heterostructure laser. To complete the processing, the wafer was first coated with oxide and patterned with openings on the mesa tops. After a zinc skin diffusion through the openings in the oxide, Au-Zn alloyed contacts were made to the p^+-InP. The wafer was then lapped from the substrate side to a thickness of $100\,\mu$m, whence a Au-Sn alloyed contact was applied. Next, Ti (200 Å) and Au (500 Å) layers were sputter deposited over the entire wafer on the mesa side to facilitate contacting. Individual BH lasers were then obtained by cleaving and saw cutting.

Five wafers have been processed for BH lasers. The active region widths of each wafer shown in Table I were obtained by measurement of mesas on a bar cleaved from one edge of that wafer. The BH lasers were tested in room-temperature pulsed operation and showed a wide range of threshold currents, the lowest values of which for each wafer are also shown in Table I.

The lowest threshold current obtained to date was 9.0 mA. Further reduction could well be achieved by using shorter devices and narrower active regions. Nevertheless, the present low thresholds are already comparable to or better than those obtained by more conventional fabrication techniques,[2–15] for which the lowest reported value was 10 mA. (Refs. 13–15). It is important to note that the new technique described here is considerably simpler than those reported previously, since it eliminates the need for the LPE regrowth of burying layers. The latter not only requires all of the special precautions for LPE regrowth but also demands critical control of layer thicknesses in order to reduce leakage current. In the present structure, the burying sidewalls of transported InP are just wide enough to provide mode confinement but narrow enough to minimize current leakage. Moreover, the InP transport has been found to be very reproducible and easily controlled.

While these initial results are highly encouraging, it should be pointed out that the yield of low threshold devices

for each wafer was only modest in this early stage of development. We feel the yield problems are due to device processing technology rather than a fundamental limitation of the present structure. For example, in the first wafer, cleaving with the mesa side up resulted in bad cleaves for the laser mirrors. This was corrected by cleaving with the substrate side up. Improved procedures for making electrical contacts with the mesa tops and for mechanically protecting the mesas are also needed.

With respect to the transport of InP, the driving force for the phenomenon is probably surface energy minimization. It is also likely that the presence of the PH_3 plays an important role in the transport process. However, detailed study of the transport kinetics has not yet been attempted, and the experimental parameters used in the present work were those for which the process was first observed. To our knowledge, this phenomenon is a novel one and may find other applications in device fabrication.

Note added in proof. Two more wafers have been processed, resulting in significant improvement in device yield and a lowest threshold current of 6.4 mA.

[1]Z. L. Liau and J. N. Walpole, Paper WB3, Technical Digest, Topical Meeting on Integrated and Guide-Wave Optics, Optical Society of America, 1982.

[2]J. J. Hsieh and C. C. Shen, Appl. Phys. Lett. **30**, 429 (1977).

[3]M. Hirao, A. Doi, S. Tsuji, M. Nakamura, and K. Aiki, J. Appl. Phys. **51**, 4539 (1980).

[4]Y. Itaya, T. Tanbun-Ek, K. Kishino, S. Arai, and Y. Suematsu, Jpn. J. Appl. Phys. **19**, L141 (1980).

[5]H. Nagai, Y. Noguchi, K. Takahei, Y. Toyoshima, and G. Iwane, Jpn. J. Appl. Phys. **19**, L218 (1980).

[6]T. Murotani, E. Oomura, H. Higuchi, H. Namizaki, and W. Susaki, Electron. Lett. **16**, 566 (1980).

[7]R. J. Nelson, R. B. Wilson, P. D. Wright, P. A. Barnes, and N. K. Dutta, IEEE J. Quantum Electron. **QE-17**, 202 (1981).

[8]S. Arai, M. Asada, T. Tanbun-Ek, Y. Suematsu, Y. Itaya, and K. Kishino, IEEE J. Quantum Electron. **QE-17**, 640 (1981).

[9]E. Oomura, T. Murotani, H. Higuchi, H. Namizaki, and W Susaki, IEEE J. Quantum Electron. **QE-17**, 646 (1981).

[10]P. C. Chen, K. L. Yu, S. Margalit, and A. Yariv, Appl. Phys. Lett. **38**, 301 (1981).

[11]W. Ng, C. S. Hong, H. Manasevit, and P. D. Dapkus, Appl. Phys. Lett. **39**, 188 (1981).

[12]W. Ng, C. S. Hong, H. Manasevit, and P. D. Dapkus, Technical Digest, Third International Conference on Integrated Optics and Optical Fiber Communicaton (Optical Society of America, 1981), p. 52.

[13]I. Mito, K. Kaede, M. Kitamura, K. Kobayashi, and S. Matsushita, see Ref. 12, p. 44.

[14]E. Oomura, H. Higuchi, R. Hirano, H. Namizaki, T. Murotani, W. Susaki, and K. Shirahata, see Ref. 12, p. 44.

[15]M. Nakamura and S. Tsuji, IEEE J. Quantum Electron. **QE-17**, 994 (1981).
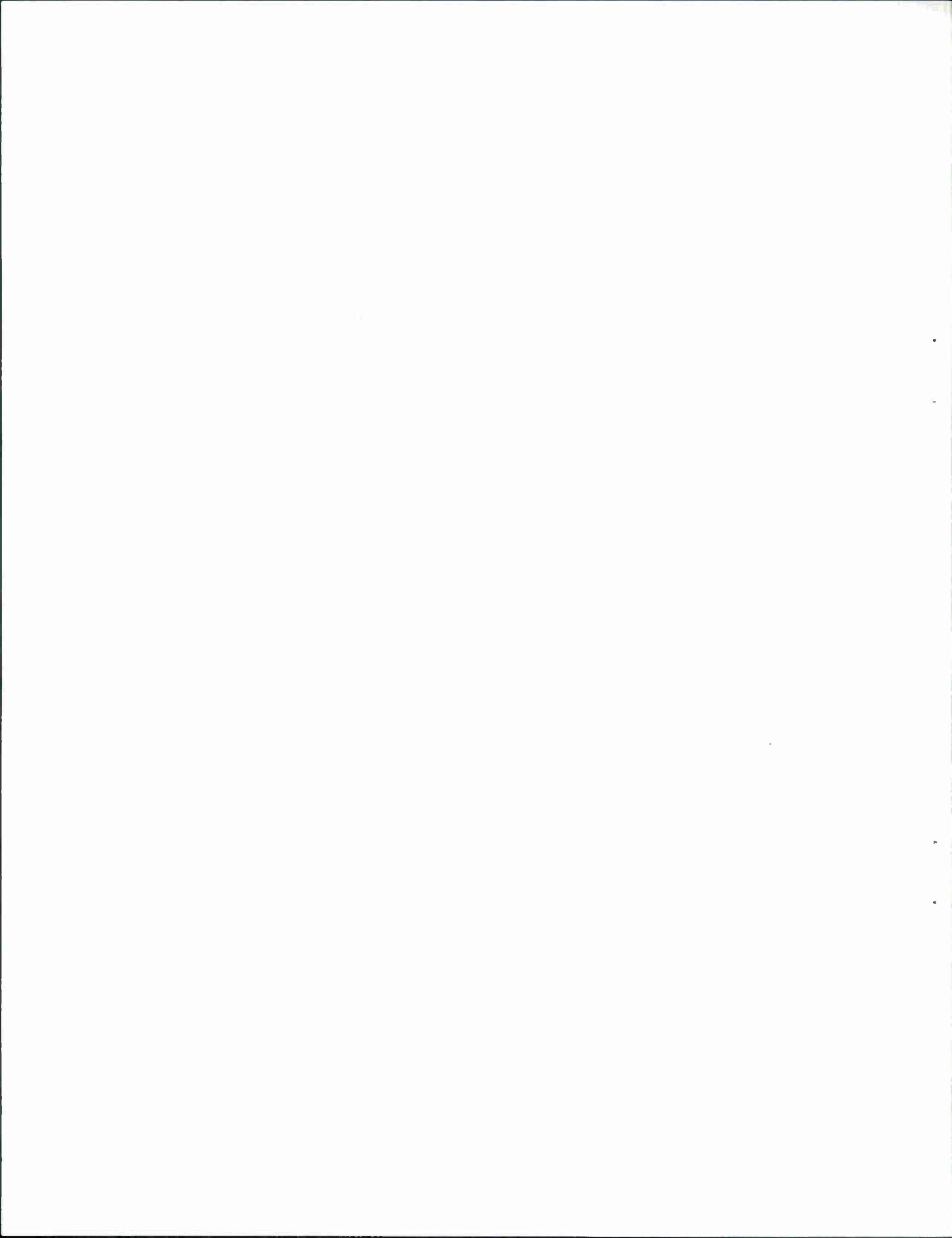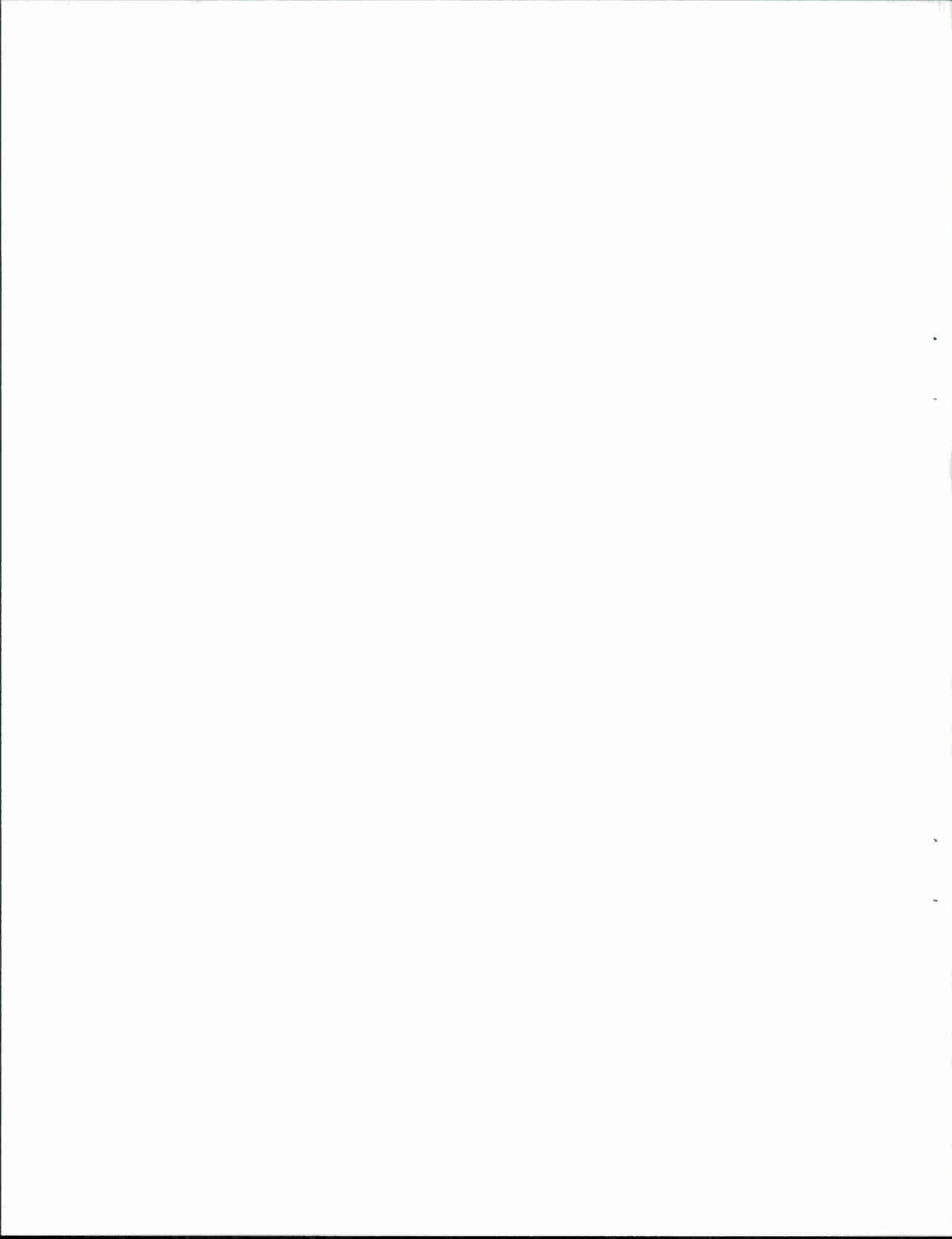
29

APPENDIX B

A Slow Selective Etch for GaInAsP Grown on InP

G. A. Ferrante, J. P. Donnelly, and C. A. Armiento

Lincoln Laboratory, Massachusetts Institute of Technology, Lexington, Massachusetts 02173

The technology for fabricating laser diodes, detectors, and optical waveguides in GaInAsP/InP epitaxial wafers requires the use of suitable etching techniques for providing smooth damage-free surfaces, precise pattern geometries, and preferential and

Key words: chemical etching, selective etch, InGaAsP, InP.

reproducible removal of specific layers. Several previous publications have reported slow controllable etches for InP (1-4) and etches for selectively removing InP layers grown over GaInAsP (5). Several etches have been used to selectively (6-9) etch GaInAsP on InP, but only a limited amount of information on etch rate and the degree of selectivity has been reported. This paper presents etch rate and surface morphology results obtained using a dilute sulfuric acid, hydrogen peroxide, and water etch, which has proven to be a slow selective etch for GaInAsP.

Slow controllable etches suitable for removing thin layers of InP are generally not usable with GaInAsP. For example, we found that iodic acid etches (2) GaInAsP in a nonuniform manner, leaving very badly pitted surfaces. Potassium-ferrocyanide potassium-hydroxide solutions, which are often used to delineate p-n junctions in the III-V compounds, etch GaInAsP faster than InP and have been used as selective etches (6, 7). The etch rates for most GaInAsP compositions tend to be fairly fast (greater than several $\mu m/min$) (7). In addition, the etch rates and resultant selectivity appear to depend on the doping of the InP and GaInAsP, as well as the composition of the etch solution, and little information on these variations has been published.

Sulfuric acid-peroxide-based etches, which are commonly used as fast polishing etches for GaAs, etch InP only slowly (10). For example, we have found that a 3 H_2SO_4:1 H_2O_2:1 H_2O solution at room temperature etches InP at about 200 Å/min. This etch (8) has been used to etch GaInAsP on InP, since the etch rate increases with increasing amounts of Ga and As in the material. A 1 H_2SO_4:6 H_2O_2:10 H_2O solution at 50°C has been used to etch mesas in GaInAs on InP (9). In both cases, details of the etch rate and selectivity were not reported. We have found that by decreasing the relative volume of H_2SO_4 compared to the standard GaAs etches and increasing that of water, while leaving that of H_2O_2 fixed, the etch rate in InP can be reduced to a negligible value while maintaining a reasonable etch rate for most GaInAsP lattice-matched compositions, except those very close to InP. As shown below, a 1 H_2SO_4:1 H_2O_2:10 H_2O solution at room temperature appears to be particularly suitable as a slow selective etch for the most commonly used GaInAsP compositions.

The samples used in these experiments were (100) liquid phase epitaxial (LPE) grown GaInAsP/InP heterojunction wafers in which the quaternary composition was either $Ga_{0.27}In_{0.73}As_{0.63}P_{0.37}$ (having a bandgap, E_g, of 0.95 eV, $\lambda = 1.3$ μm), $Ga_{0.17}In_{0.83}As_{0.59}P_{0.61}$ ($E_g = 1.08$ eV, $\lambda = 1.15$ μm), or $Ga_{0.10}In_{0.90}As_{0.04}P_{0.96}$ (E_g 1.24 eV, $\lambda = 1.04$ μm). Each etch solution used was placed in a clean 200 ml Pyrex beaker which was modified for mounting a microscope slide inside. Since a great deal of heat is generated when sulfuric acid etches are mixed, some care must be taken to insure that the solution returns to room temperature, 21° ± 1°C, before etching samples. If this is not done, higher etch rates than reported in this paper will be obtained. The solution was stirred continuously by means of a Teflon-coated magnetic stirrer. Part of each sample to be etched was masked with SiO_2 to provide a step in order to measure etch depth. For etching, the sample was mounted on a microscope slide using Apiezon wax. After etching, the mask was removed, the sample rinsed, dried, and inspected. The etch depth was measured with a Dek-tak surface profiler.

The etch depth *vs.* etch time obtained on a (100) $Ga_{0.27}In_{0.73}As_{0.63}P_{0.37}$ ($\lambda = 1.3$ μm) sample in a 1 H_2SO_4:1 H_2O_2:10 H_2O room temperature solution is shown in Fig. 1. As determined from this data, the etch rate is a very constant 1000 Å/min. The etched GaInAsP surface appeared to be free of any etch
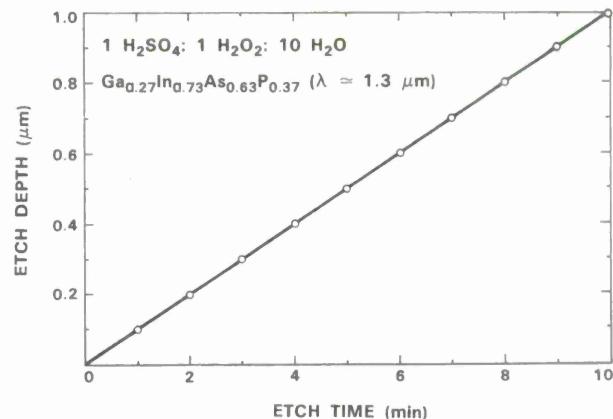

Fig. 1. The etch depth vs. etch time obtained on a $Ga_{0.27}In_{0.73}As_{0.63}P_{0.37}$ ($\lambda = 1.3$ μm) layer etched in a room temperature 1 H_2SO_4:1 H_2O_2:10 H_2O solution.

$Ga_{0.27}In_{0.73}As_{0.63}P_{0.37}$
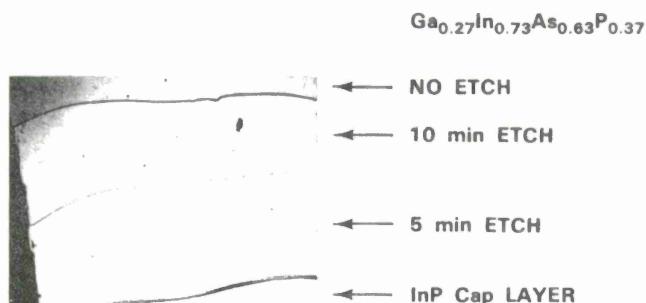
Fig. 2. Photomicrograph of a $Ga_{0.27}In_{0.73}As_{0.63}P_{0.37}$/InP double heterojunction wafer in which most of the top InP was removed in concentrated HCl and different areas of the quaternary layer etched for the times indicated (no etch, 5 min etch and 10 min etch) in a 1 H_2SO_4:1 H_2O_2:10 H_2O solution.

related defects. Figure 2 shows a photomicrograph of a double heterojunction wafer in which the top InP layer was removed from most of the wafer using concentrated HCl, a selective etch which etches (100) InP at 5.4 $\mu m/min$ while having a negligible etch rate on 1.3 μm bandgap GaInAsP. Different areas of the GaInAsP layer were then etched for different times using 1 H_2SO_4:1 H_2O_2:10 H_2O. The etched surfaces have the same surface texture as the originally exposed quaternary surface.

Table I lists the etch rate measuered for several different GaInAsP compositions and InP. The errors in the etch rates are estimated to be less than ±10 Å/min. For (100) $Ga_{0.17}In_{0.83}As_{0.59}P_{0.61}$ ($\lambda ± 1.15$ μm), the etch rate is 420 Å/min, while for (100) $Ga_{0.10}In_{0.90}As_{0.04}P_{0.96}$ ($\lambda = 1.04$ μm), the etch rate decreases further to 75 Å/min. The etch depth on (100) InP could not be measured after an hour's etch time although a fine demarcation line between the etched and unetched areas of the samples was observed. The surface quality of the InP exposed to the dilute sulfuric acid etch was good (see InP surface in Fig. 2, which was exposed to the dilute sulfuric acid etch). The same result was obtained on (100)-oriented liq-

Table I. Etch rate of InP and various compositions of GaInAsP in a 1 H_2SO_4:1 H_2O_2:10 H_2O solution at room temperature

Material	Etch rate
(100) $Ga_{0.27}In_{0.73}As_{0.63}P_{0.37}$ ($\lambda = 1.3$ μm)	1000 Å/min
(100) $Ga_{0.17}In_{0.83}As_{0.59}P_{0.61}$ ($\lambda = 1.15$ μm)	420 Å/min
(100) $Ga_{0.10}In_{0.90}As_{0.04}P_{0.96}$ ($\lambda = 1.04$ μm)	75 Å/min
(100) InP	Negligible
(111)B InP	30 Å/min

uid encapsulated Czochralski (LEC) InP samples doped with either Zn and Sn to concentrations greater than 10^{18} cm^{-3}. On (111)B InP, however, an etch rate of $\approx$30 A/min was measured. The higher etch rate on the (111)B plane is consistent with the results reported in Ref. (9).

In conclusion, a room temperature solution of 1 H_2SO_4:1 H_2O_2:10 H_2O etches (100) InP at a negligible rate while it etches most lattice-matched compositions of GaInAsP at a reasonable rate leaving a good surface morphology. This etch should prove useful as a slow selective etch in a variety of applications.

Acknowledgments

The authors would like to thank S. H. Groves, Z. L. Liau, M. C. Plonko, and D. E. Mull for supplying the GaInAsP layers used in these experiments. This work was sponsored by the Department of the Air Force.

Manuscript submitted Oct. 5, 1982; revised manuscript received Dec. 14, 1982.

Any discussion of this paper will appear in a Discussion Section to be published in the December 1983 JOURNAL. All discussions for the December 1983 Discussion Section should be submitted by Aug. 1, 1983.

REFERENCES

1. R. Becker, *Solid-State Electron.*, **16**, 1241 (1973).
2. A. R. Clawson, D. A. Collins, D. I. Elder, and T. J. Monroe, NOSC Technical Note 592, Naval Ocean Systems Center, San Diego, California, Dec. 13, 1978.
3. S. Adachi and H. Kawaguchi, *This Journal*, **128**, 1342 (1981).
4. S. Adachi, H. Kawaguchi, and G. Iwane, *J. Mater. Sci.*, 16, 2449 (1981).
5. S. B. Phatak and G. Kelner, *This Journal*, **126**, 287 (1979).
6. Z. L. Liau and J. N. Walpole, *Appl. Phys. Lett.*, **40**, 56 (1982).
7. K. L. Conway, A. G. Dentai, and J. C. Campbell, *J. Appl. Phys.*, **53**, 1836 (1982).
8. J. J. Hsieh and C. C. Shen, *Appl. Phys. Lett.*, **30**, 429 (1977).
9. T. P. Pearsall and M. Papuchon, *ibid.*, **33**, 640 (1978).
10. Y. Nishitani and T. Kotani, *This Journal*, **126**, 2269 (1979).
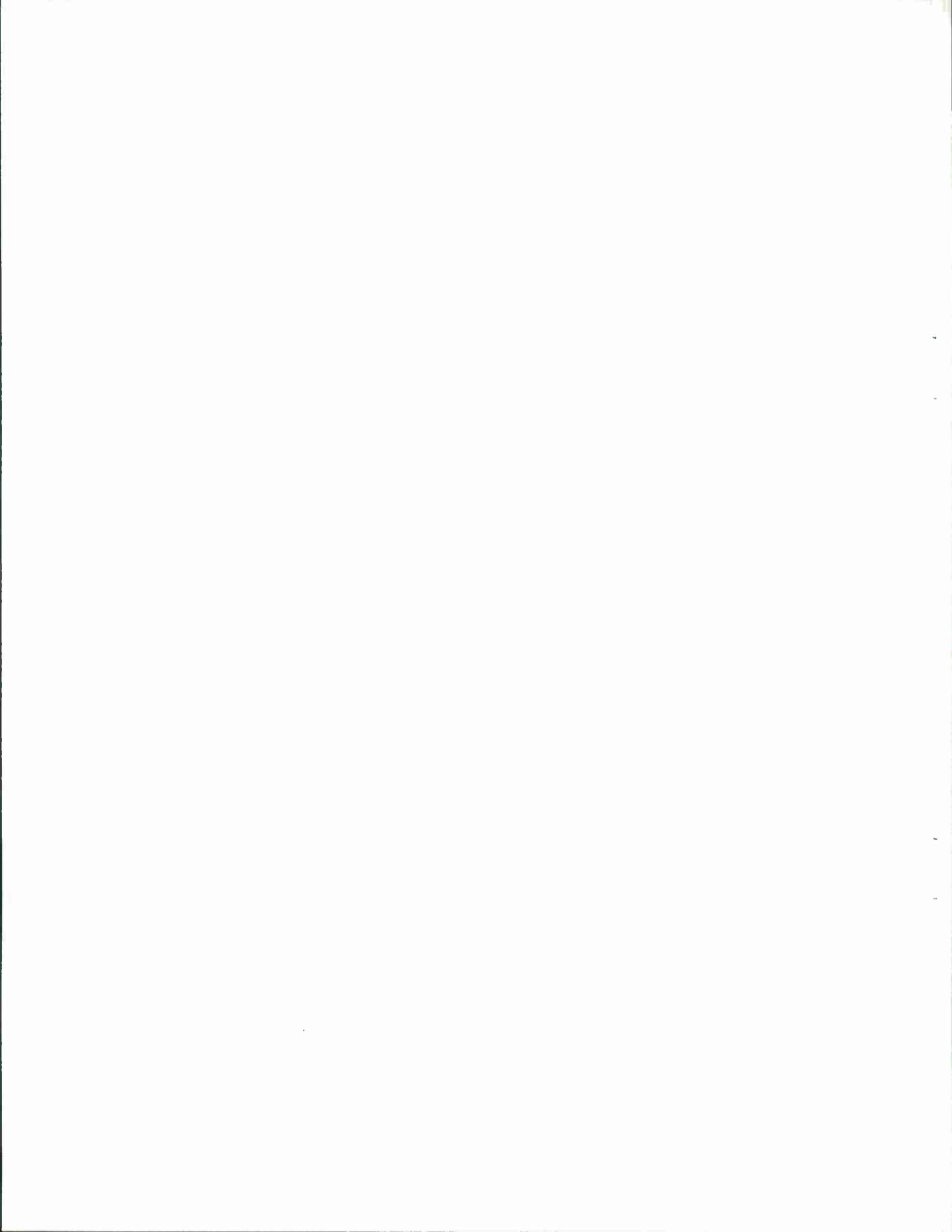
APPENDIX C
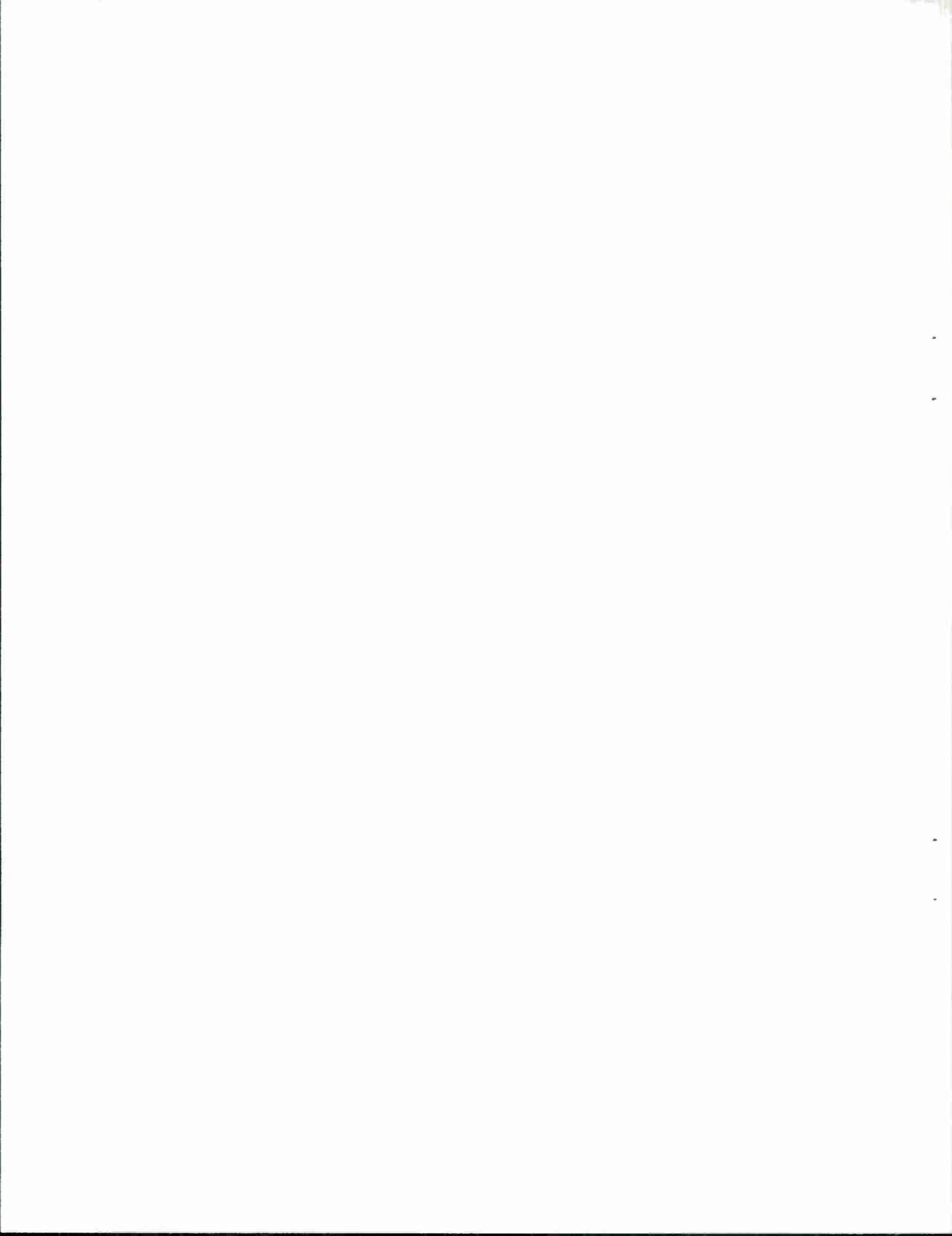
Three-Guide Optical Couplers in GaAs

JOSEPH P. DONNELLY, MEMBER, IEEE, NICHOLAS L. DeMEO, JR., AND GUISEPPE A. FERRANTE

Abstract—Three-guide optical couplers consisting of three 4.75-μm-wide slab-coupled rib guides separated by 4.25 μm have been fabricated in GaAs. The performance of these couplers at 1.28 μm is in close agreement with that predicted using a modified effective-index method to obtain an approximate analytical solution for this type of coupler. The coupling length needed to symmetrically transfer power from the center guide to the two outside guides was 3.2 mm. At this length, less than 1 percent of the power remained in the center guide. The length needed to transfer power from one outside guide to the other outside guide was ≈ 6.4 mm, which is $\approx \sqrt{2}$ times that of a similar two-guide coupler and twice that required to couple power from the center guide to the two outside guides. The power transfer efficiency in this case is not as good as when power was inputted into the center guide. Three-guide couplers of this type should prove useful as power dividers and combiners, especially in cases where waveguide bend losses preclude the use of "Y"-junctions. They may also prove useful as replacements for two-guide couplers where either sharper transfer characteristics are desired or where losses due to waveguide bends are again unacceptable.

I. INTRODUCTION

OPTICAL COUPLERS are an important component of almost all integrated optical circuit concepts. There has been a fair amount reported on two-guide optical couplers

including experimental results on couplers fabricated on GaAs [1]–[9], InP [10], and GaInAsP [11]. Work reported to date on three-guide couplers has been theoretical [12], [13]. When used to couple power from one outside guide to the other outside guide, the three-guide coupler has sharper transfer characteristics than a similar two-guide coupler and it has been proposed to use this feature for improved sampling and filtering [13]. Another possible application of three-guide couplers is their use as symmetrical power dividers and combiners. In this paper, we first discuss a three-guide optical coupler theory applicable to our experimental structures and then present experimental results on three-guide couplers comprised of equally spaced slab-coupled rib waveguides, in GaAs. A comparison with two-guide couplers fabricated on the same wafer will also be given.

II. THEORY

The symmetrical three-guide couplers used in these experiments are composed of three slab-coupled rib waveguides in close proximity as shown in Fig. 1(a). The individual waveguides were designed to be single mode [14] and consist of a rib etched in a nominally undoped n⁻-GaAs epitaxial layer grown on an n⁺-GaAs substrate. Details of the fabrication are given later in the paper. As indicated in Fig. 1(b), the refractive index of the epilayer n_1, is higher than that of the substrate n_2,

(a)

(b)
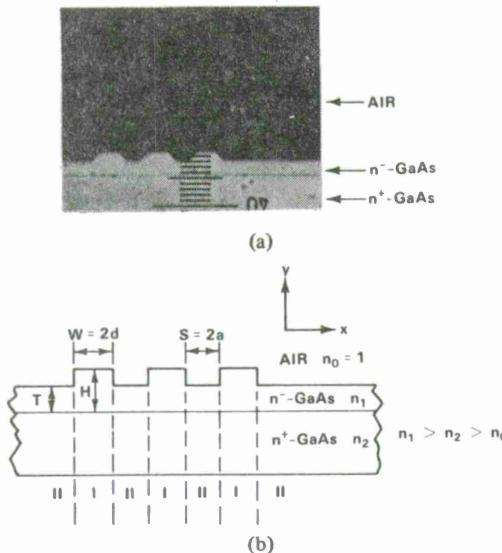
Fig. 1. (a) Photomicrograph of cleaved cross section of GaAs three-guide coupler. The sample has been treated with a stain/etchant to reveal the n^--n^+ interface. The scale on the photomicrograph is 1 μm/div. (b) Schematic cross section of three-guide coupler with rectangular ribs of a width equal to the average width (same cross-sectional area) of the actual guides. The regions I and II are modeled as slab waveguides to determine the effective guide index in different portions of the n^--layer.

which in turn is higher than air $n_0 = 1$. The width W of the rib shown in Fig. 1(b) is the average width of the experimental trapezoidal ribs, i.e., the areas of the ribs are the same [14].

Since an exact analysis of these three-guide couplers is not possible, an extension of the effective-index method [15], [16] has been used to obtain an approximate analytic solution and some insight into device behavior. Using this method, the coupler is divided into regions I and II, as shown in Fig. 1(b), and each region is assumed to be a slab guide of infinite extent in the x-direction. Specifically, region I is assumed to be a three-layer slab guide consisting of an n^+-substrate, an n^--epilayer of thickness H, and air ($n_0 = 1$), while region II is assumed to be a similar three-layer slab with n^--epilayer thickness T. The effective guide indexes, n_{g_I} and $n_{g_{II}}$, are then obtained by calculating the propagation constant or phase velocity $\beta_{I, II} = 2\pi n_{g_{I, II}}/\lambda$ (where λ is the wavelength of light) for the lowest order mode for each slab waveguide (both regions only supported a single mode in the experimental couplers) using the usual asymmetrical three-layer slab guide eigenvalue equation [17], [18]. Since the experimental data presented later in this paper was obtained with quasi-TE modes, i.e., the major transverse electric field component was in the x-direction (see Fig. 1), the solution appropriate for TE modes was used in this part of the problem.

The coupler was then analyzed by modeling it as a seven-layer structure of infinite extent in the y-direction with index n_{g_I} in the guiding regions and $n_{g_{II}}$ outside the guiding regions, as shown in Fig. 2(a). This part of the analysis follows that given by Iswaki et al. [12] who analyzed the slab waveguide case for TE modes. The width of the guide is $W = 2d$ and the separation between guides is $S = 2a$. If the individual isolated guides are single moded, this three-guide coupler has three normal modes, as depicted in Fig. 2(b). Letting K be the
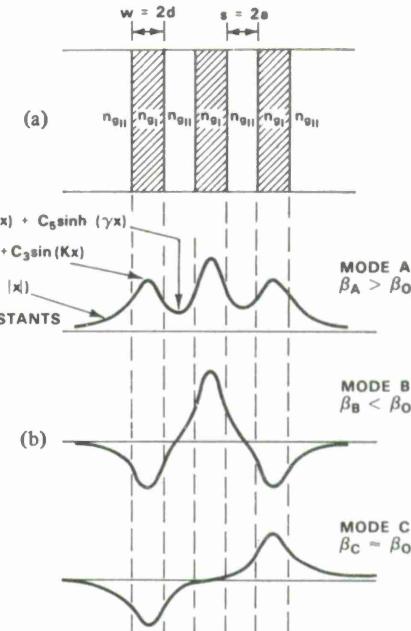
Fig. 2. (a) Effective-index model of the three-guide coupler. (b) Three normal modes of the three-guide coupler.

transverse wavenumber (in the x-direction) of the fields in the guides and γ the transverse attenuation coefficient in the surrounding media (as indicated in Fig. 2(b)), the eigenvalue equation for each mode can be found from the set of equations obtained by equating the tangential field components at each boundary. The calculation can be significantly simplified by using the symmetry of the modes. For the two symmetric modes (modes A and B), the resulting eigenvalue equation is

$$\frac{(K \tan Kd - r\gamma)^2 (K + r\gamma \tan Kd)}{(K \tan Kd + r\gamma)(K^2 + r^2\gamma^2) \tan Kd} = e^{-4\gamma a} \qquad (1)$$

where $r = 1$ for TE modes and $r = (n_{g_I}/n_{g_{II}})^2$ for TM modes. Since the major transverse component of the electric field for the experimental data is in the x-direction, it is appropriate to use the solution for TM modes in this part of the problem. (Note that for these slab-coupled guides $r \approx 1$ even for TM modes, so there is little difference between the TE and TM solution.) The attenuation coefficient γ and propagation constant or phase velocity β of the fields are related to K by

$$\gamma = (k_1^2 - k_2^2 - K^2)^{1/2} \qquad (2)$$

and

$$\beta = (k_1^2 - K^2)^{1/2} \qquad (3)$$

where $k_{1,2} = (2\pi/\lambda) n_{g_{I, II}}$.

Equation (1) has two solutions, one corresponding to the A mode and one corresponding to the B mode (see Fig. 2(b)). For the A mode

$$K_A < K_0, \gamma_A > \gamma_0$$

and

$$\beta_A > \beta_0$$

where the A subscript represents values appropriate to the A mode and the 0 subscript represents values appropriate to the mode of a single isolated slab guide of index n_{g_I} in the guiding region and $n_{g_{II}}$ outside the guiding region [11], [16], [17]. For the B mode

$$K_B > K_0, \gamma_B < \gamma_0$$

and

$$\beta_B < \beta_0$$

where the B subscript represents values appropriate to the B mode.

For the antisymmetric mode (mode C), the eigenvalue equation is

$$\frac{(K \tan Kd - r\gamma)(K + r\gamma \tan Kd)^2}{(K - r\gamma \tan Kd)(K^2 + r^2\gamma^2) \tan Kd} = e^{-4\gamma a}. \tag{4}$$

This equation has one solution. The propagation constant of the C mode, β_C, can either be larger or smaller than β_0 depending on guide parameters, but the difference $|\beta_C - \beta_0|$ is much smaller than $\beta_A - \beta_0$ or $\beta_0 - \beta_B$.

For loose coupling, i.e., when $\exp(-2\gamma_0 a)$ is small, the phase velocities of the modes are only slightly perturbed from those of a single isolated guide.

In this case, $\beta \approx \beta_0 \pm \Delta$ and, therefore, $K \approx K_0 \mp \Delta\beta_0/K_0$ and $\gamma \approx \gamma_0 \pm \Delta\beta_0/\gamma_0$. Substituting K and γ into (1), (2), and (3), we obtain

$$\beta_A = \beta_0 + \Delta \tag{5a}$$

$$\beta_B = \beta_0 - \Delta \tag{5b}$$

where

$$\Delta = \frac{\sqrt{2}\, rK_0^2 \gamma_0^2}{\beta_0 [r(K_0^2 + \gamma_0^2) + (K_0^2 + r^2\gamma_0^2)\gamma_0 d]} \exp(-2\gamma_0 a). \tag{6}$$

It should be noted that Δ is $\sqrt{2}$ times larger than the change in phase velocities obtained when the same type analysis is performed on a similar two-guide coupler [12].

Similarly

$$\beta_C = \beta_0 + \sigma \tag{7}$$

where

$$\sigma = \frac{rK_0^2\gamma_0^2 (K_0^2 - r^2\gamma_0^2) \exp(-4\gamma_0 a)}{\beta_0(K_0^2 + r^2\gamma_0^2)[r(K_0^2 + \gamma_0^2) + (K_0^2 + r^2\gamma_0^2)\gamma_0 d]}. \tag{8}$$

Note that σ is much smaller than Δ and can usually be neglected. If σ is neglected, the results are the same as those obtained using the coupled-mode theory [13], which neglects the coupling between the two outside guides.

To see how the three-guide coupler will work under various inputs, two cases will be examined: 1) input power into the center guide and 2) input power into one of the outside guides.

With power input into the center guide, only the A and B modes are excited, such that at $z = 0$, their fields are in-phase, i.e., additive in the center guide and subtractive in the outside guides. Since A and B have different phase velocities, at some point z down the guide they will be 180° or π rad out of phase, i.e., their fields will be subtractive in the center guide and addi-

tive in the two outside guides. This occurs at multiples of the coupling length, which is given by

$$L_{CT \to 0} = \frac{\pi}{(\beta_A - \beta_B)}. \tag{9}$$

In the loose coupling approximation $(\beta_A - \beta_B) = 2\Delta$ and

$$L_{CT \to 0} \approx \frac{\pi}{2\Delta}. \tag{10}$$

The power in each guide as a function of distance down the guide can be calculated in a straightforward manner. The result in the general case, however, is somewhat complex. Without going into this detail, insight into the three-guide coupler can be gained by assuming that the transverse field shapes of the two modes in the individual guides are not perturbed significantly from those of a single isolated guide. This assumption is less stringent than that required for true loose coupling, i.e., when (5) to (8) are valid. With this assumption, the powers in the center guide P_{CT} and the two outside guides, P_{01} and P_{02}, as a function of distance are given by

$$P_{CT} \approx P_{IN} \cos^2\left(\frac{\beta_A - \beta_B}{2}\right) z \tag{11a}$$

and

$$P_{01} = P_{02} \approx (P_{IN/2}) \sin^2\left(\frac{\beta_A - \beta_B}{2}\right) z \tag{11b}$$

where P_{IN} is the input power to the center guide. In the true loose-coupling case, $\Delta = (\beta_A - \beta_B/2)$ can be substituted in (11a) and (11b).

Note that since the shapes of the two modes are perturbed from those of a single isolated guide, complete cancellation between modes in any guide is never possible but only a good approximation. The looser the coupling, the more accurate the approximation, but also the longer the coupling length (at least over most of the range (11a) and (11b) are valid). Some compromise between power transfer efficiency and coupling length is possible when the three-guide coupler is used with power input to the center guide.

Since these couplers are bilateral, equal in-phase inputs to the outside guide will result in power transferring to the center guide in a coupling length. Symmetrical three-guide couplers can, therefore, be used as both power dividers and combiners, with characteristics similar to "Y"-junctions.

With excitation to the center guide, the power division equations are qualitatively the same as those obtained for a symmetrical two-guide coupler except that in the case of the two-guide couplers, all the coupled power is contained in the single-coupled guide. Since, in the loose-coupling case, Δ for the three-guide couplers is $\sqrt{2}$ times larger than that of a two-guide coupler, the coupling length $L_{CT \to 0}$ is shorter than that of a two-guide coupler by a factor of $1/\sqrt{2}$.

With input power into one of the outside guides of a three-guided coupler, the situation is more complex. At $z = 0$, modes A and B are excited out of phase such that they are subtractive in the center guide and additive in the two outside guides. Mode C is excited so it is additive to the sum of modes A and B in the input outside guide and subtractive in the other out-

41
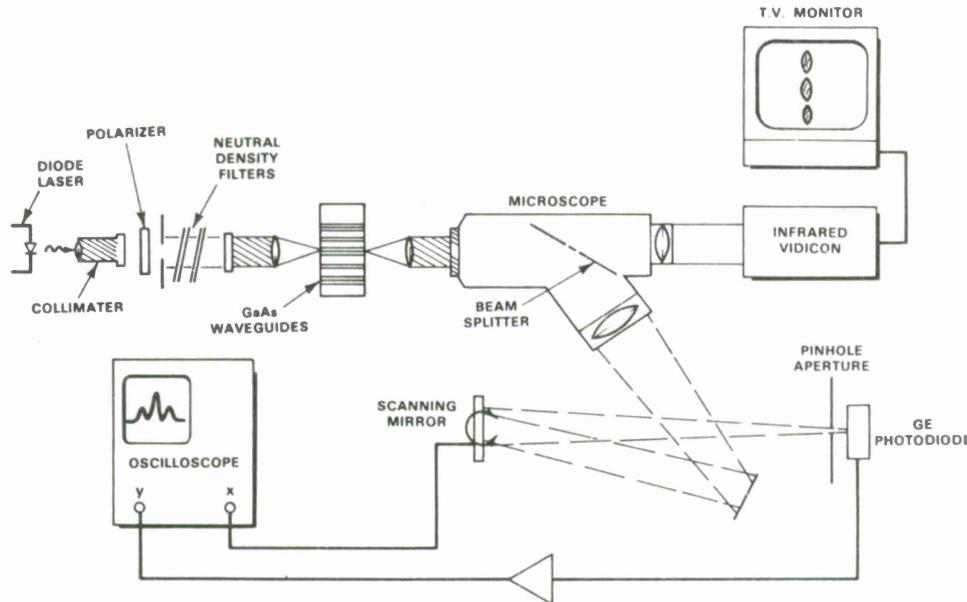
Fig. 3. Experimental setup for evaluating the three-guide couplers.

side guide. Again assuming that the shapes of the different modes in the individual guides are not perturbed significantly from those of a single isolated guide, the powers in the input outside guide P_{01}, the center guide P_{CT}, and the coupled outside guide P_{02}, are given approximately by

$$P_{01} = \left(\frac{P_{IN}}{4}\right)\left[1 + \cos^2\left(\frac{\beta_A - \beta_B}{2}\right)z + \cos(\beta_A - \beta_C)z\right.$$
$$\left. + \cos(\beta_C - \beta_B)z\right] \tag{12a}$$

$$P_{CT} = \left(\frac{P_{IN}}{2}\right)\sin^2\left(\frac{\beta_A - \beta_B}{2}\right)z \tag{12b}$$

$$P_{02} = \left(\frac{P_{IN}}{4}\right)\left[1 + \cos^2\left(\frac{\beta_A - \beta_B}{2}\right)z - \cos(\beta_A - \beta_C)z\right.$$
$$\left. - \cos(\beta_C - \beta_B)z\right]. \tag{12c}$$

To obtain good beats in the outside guides with distance down the coupler, the phase velocities of the three modes must be related to each other in some simple fashion. This is true in the loose-coupling case, where $\beta_A \approx \beta_0 + \Delta$, $\beta_B \approx \beta_0 - \Delta$ and $\beta_C \approx \beta_0$. The powers in the three guides are then given approximately by

$$P_{01} \approx (P_{IN}/4)(1 + \cos \Delta z)^2 = P_{IN} \cos^4(\Delta z/2) \tag{13a}$$

$$P_{CT} \approx (P_{IN}/2)\sin^2 \Delta z \tag{13b}$$

$$P_{02} \approx (P_{IN}/4)(1 - \cos \Delta z)^2 = P_{IN} \sin^4(\Delta z/2). \tag{13c}$$

With this approximation, power is transferred from the input outside guide to the coupled outside guide in a length

$$L_{01 \to 02} = \pi/\Delta. \tag{14}$$

This coupling length is twice that required to symmetrically transfer power from the center guide to the two outside gudes and is $\sqrt{2}$ times that required for power transfer in a two-guide coupler [11], [12]. Since there are three modes involved, this

approximation, valid only for loosely coupled guides, is not expected to be as good as for the case where power is input into the center guide.

III. FABRICATION

As previously noted, the symmetric three-guide couplers studied in this work were fabricated entirely in GaAs and comprised of three closely spaced slab-coupled rib waveguides etched in an n^--GaAs epilayer on an n^+-GaAs substrate. The waveguides were fabricated by growing an unintentionally doped GaAs layer by standard vapor-phase epitaxial technique on a (100)-oriented 2×10^{18} cm^{-3} n^+-substrate. The epitaxial layer was n-type with a carrier concentration of 1×10^{15} cm^{-3} and had a thickness of 4.2 μm. The ribs or guides were formed by first defining stripes in a $\approx$300-Å evaporated Ti layer using standard photolithographic and liftoff techniques. For the guides reported in this paper, the stripes were oriented along a $(0\,\bar{1}\,\bar{1})$ direction. Stripes for symmetric three-guide couplers, two-guide couplers and single isolated guides were intermixed on the wafer for testing purposes. The n^--epitaxial layer was then etched, using the Ti as an etch mask, in a cooled 1 H_2SO_4 : 8 H_2O_2 : 1 H_2O solution to an etch depth of 1.5 μm [19], resulting in single-mode operation of the single isolated guides. The Ti was then removed in buffered HF. A resultant three-guide coupler is shown in Fig. 1(a). Note that due to undercutting the ribs are actually trapezoidal in shape. The mean width of a rib is 4.75 μm and the mean spacing or separation between ribs is 4.25 μm. After the ends were cleaved, the sample was mounted on a high-performance translation-rotary stage for optical evaluation. Following evaluation at one length, the sample was cleaved to a shorter length and the evaluation repeated.

IV. EXPERIMENTAL PROCEDURES

The experimental setup used to test the couplers is shown in Fig. 3. Measurements were made using an end-fired coupling scheme [4]. Radiation from a single-mode CW GaInAsP/InP
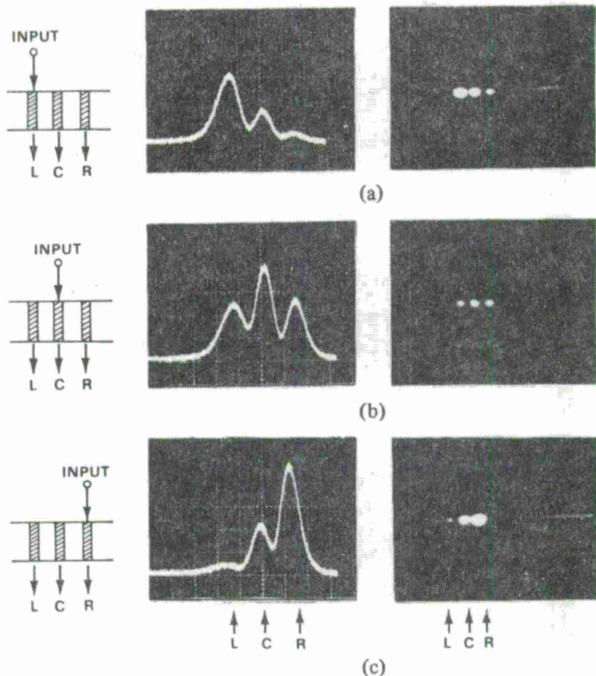
Fig. 4. Typical outputs obtained on the oscilloscope and TV monitor for a three-guide coupler with (a) input power into the left outside guide, (b) input power into the center guide, and (c) input power into the right outside guide. The length of the guide was 1.7 mm.


Fig. 5. (a) Relative output power out of each guide as a function of length for a three-guide coupler with input power into the center guide. (b) The outputs obtained on the oscilloscope and TV monitor for a length of 3.2 mm.

double-heterojunction laser operating at 1.28 μm was collimated, passed through a polarizer, aperture, and neutral density filter and focused on the cleaved input face of the waveguide sample using a microscope objective. The electric field of the input light was polarized parallel to the plane of the slab. The input from the waveguide sample was focused by a beam-splitting microscope into two images. One output image went to an infrared TV camera system and the other image was passed through a pin-hole aperture onto a Ge photodiode. The output image could either be scanned across the pin-hole aperture using a scanning mirror or the aperture could be precisely translated across the image. When the scanning mirror was used, the output of the Ge detector could be displayed on an oscilloscope as a function of effective position. For purposes of comparison, single isolated guides and three-, and two-guide couplers were evaluated. For the three-guide couplers, measurements were taken with the input power focused sequentially on the center guide and both outside guides. Fig. 4 shows typical results obtained on a three-guide coupler. This coupler had a length of 1.7 mm. Fig. 4(a), 4(b), and 4(c) show the outputs obtained for power into the left outside guide, the center guide, and the right outside guide, respectively. The output observed on the oscilloscope using the scanning mirror is shown on the left, while the picture observed in the TV monitor is shown on the right. Note that the scanned mirror system introduces a slight asymmetry making the output of the left guide look slightly wider and lower than the output of the right outside guide.

V. RESULTS

For the isolated single guides, a single intensity maximum was observed under the rib as expected, since the guides were designed for single-mode operation [14]. Measurements in-

dicated that the loss in the three-guide couplers was, within experimental error (±0.2 cm^{-1}), the same as that of the single isolated guides, and at 1.28 μm was about 1 cm^{-1}.
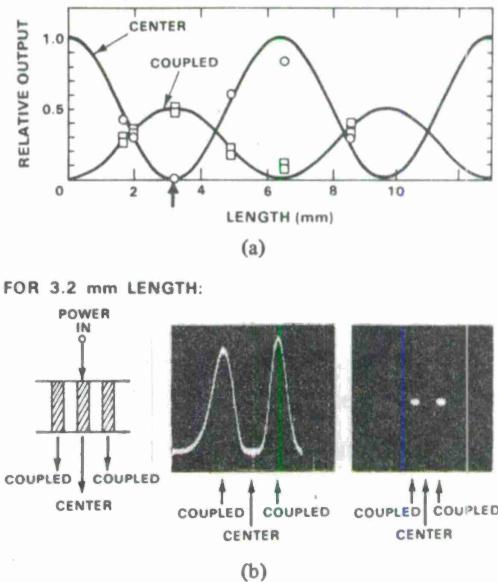
The outputs of the two- and three-guide couplers as a function of length were in good agreement with that expected from theory. The best fit to the experimental data gave a coupling length for symmetrically transferring power from the center guide of a three-guide coupler to the two outside guides $L_{CT \to 0}$ of $\approx$3.2 mm. Fig. 5(a) shows the relative power out of each guide of a three-guide coupler versus length for power input into the center guide. Also shown (Fig. 5(b)) is the oscilloscope and the TV output obtained for a length of 3.2 mm. Most of the asymmetry in the oscilloscope photograph is due to the scanning optics, as previously mentioned. The solid curves in Fig. 5(a) are plots of (11(a)) and (11(b)) for $\Delta \approx (\beta_A - \beta_B/2) = (\pi/2)/(3.2 \text{ mm})$. The relative power out of all three guides is a reasonably good fit to the approximate power division equations. At a length of 3.2 mm, the power input to the center guide is divided between the two outside guides, with minimal power ($\leqslant$1 percent) remaining in the center guide.

Using the effective-guide-index method described in Section II, the coupling length to transfer power from the center guide to the two outside guides $L_{CT \to 0}$ was calculated to be 2.85 mm using the loose-coupling approximation in (6) and (10) and 2.79 mm using the more exact approximation in (1) and (9). In these calculations, the average width of the trapezoidal ribs, 4.75 μm, and average spacing, 4.25 μm, were used [14]. The effective index of the epitaxial layer n_1 was taken [20] as 3.43 and the usual free-carrier effect on index was used to determine the index of the n$^+$-substrate n_2. The agreement between the calculated and experimental coupling lengths is quite good ($\approx$12.5-percent difference). It is not clear how much of the difference is due to inherent limitations in the effective-guide-index calculation and how much is due to the use of inaccurate waveguide parameters. Using values obtained from the effective-guide-index method, it would appear that

43
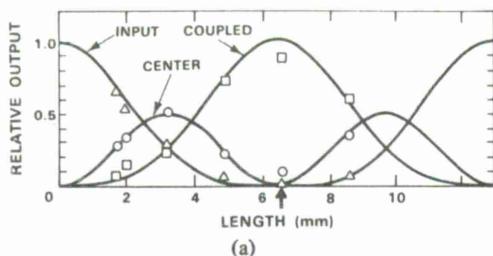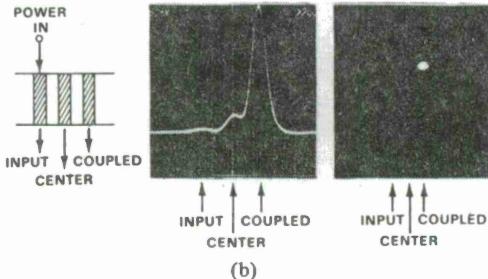
Fig. 6. (a) Relative output out of each guide as a function of length for a three-guide coupler with input power into one of the outside guides. (b) The outputs obtained on the oscilloscope and TV monitor for a length of 6.5 mm.


Fig. 7. (a) Relative output power of each guide as a function of length for a two-guide coupler. (b) The outputs obtained on the oscilloscope and TV monitor for a length of 4.9 mm.

the guides can be considered only marginally loosely coupled since exp $(-2\gamma_0 a) \approx 0.18$ and the more exact differences in β, $(\beta_A - \beta_0)$ and $(\beta_0 - \beta_B)$ differ by about 20 percent. The slightly longer experimental coupling length means that the coupling between guides is slightly less (≈ 12.5 percent) than calculated. Furthermore, the good power transfer from the center guide to the two outside guides indicates that the power equations (11a) and (11b) are good approximations for this input case.

Fig. 6(a) shows the relative power out of each guide of the same three-guide coupler versus length for power into an outside guide. Also shown are the oscilloscope and TV outputs at a length of 6.5 mm (Fig. 6(b)). The solid lines in Fig. 6(a) are plots of (13a), (13b), and (13c) with the same Δ as used in Fig. 5. The coupling length in the loose coupling approximation for complete power transfer from one outside guide to the other should be 6.4 mm. The data obtained at a length of 6.5 mm, which is slightly longer, shows most of the power in the coupled outside guide (≈ 86 percent), a small amount of power in the center guide (≈ 11.5 percent), and only ≈ 2.5 percent in the input outside guide. Since in this case there are three modes whose phase velocities are really not exactly related to each other in a simple way (only an approximation for loose coupling), the beats between these modes and, therefore, the power transfer is not expected to be as good as in the case where power was input into the center guides. It is not completely clear, however, why there is so much residual power in the center guide at a length of 6.5 mm. There is, nevertheless, fairly good overall agreement between the measured relative powers and plots of (13a), (13b), and (13c). As mentioned above, the actual coupling between guides is slightly less than calculated using the effective-guide-index method and it appears that even in this input case the guides at least to first order may be considered loosely coupled.

For comparison purposes, Fig. 7(a) shows the relative output of each guide of a two-guide coupler versus length. Also shown
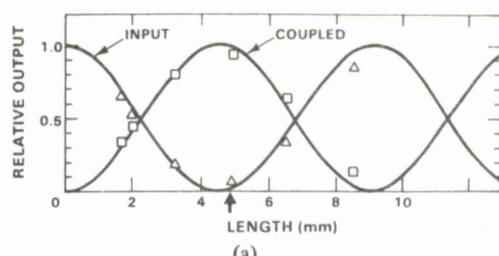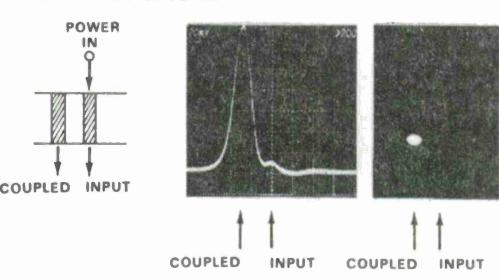
are the oscilloscope and TV outputs at a length of 4.9 mm. The solid line represents the power division equations of a two-guide coupler with a coupling length $\sqrt{2}$ times larger than that of a three-guide coupler with power input into the center guide. At a length of 4.9 mm, which is somewhat longer than the 4.5-mm coupling length, there is still almost complete power transfer from one guide to another.

Although the length required to transfer power from one outside guide to the other of a loosely coupled three-guide coupler (Fig. 6) is $\sqrt{2}$ times larger than that of a similar two-guide coupler (Fig. 7), note that (as long as it is acceptable to dump any residual power in the center guide) the length necessary to obtain a good power transfer ratio between the power in the two outside guides is less critical in the three-guide coupler. This results from the fact that the ratio of the power in the coupled guide to that in the input guide goes as $\tan^4 (\Delta z/2)$ for the three-guide coupler and only as $\tan^2 (\Delta z/\sqrt{2})$ for the two-guide coupler. To take advantage of this "sharper" characteristic, however, the guides must be loosely coupled and the restriction on coupling for the loose-coupling approximation to be valid are more severe in this case than in the case of a two-guide coupler or when the three-guide coupler is used as a power divider or coupler (since only two modes are involved in this latter case).

To give some indication of the similarity between couplers on a wafer, Fig. 8 shows the scanned output oscilloscope traces for two different three-guide couplers (#27 and #30) with input into Fig. 8(a) the left outside guide, (b) the center guide, and (c) the right outside guide. The sample length is 4.9 mm. Only the relative magnitudes of the three peaks in each picture are of significance since no effort was made to keep the absolute value of the power coupled into the three-guide couplers constant for each input. As can be seen in the figure, the relative outputs (i.e., the output in each guide divided by the total output) of the two couplers are in substantial agreement for each input. In addition, at a length of 3.2 mm the output power
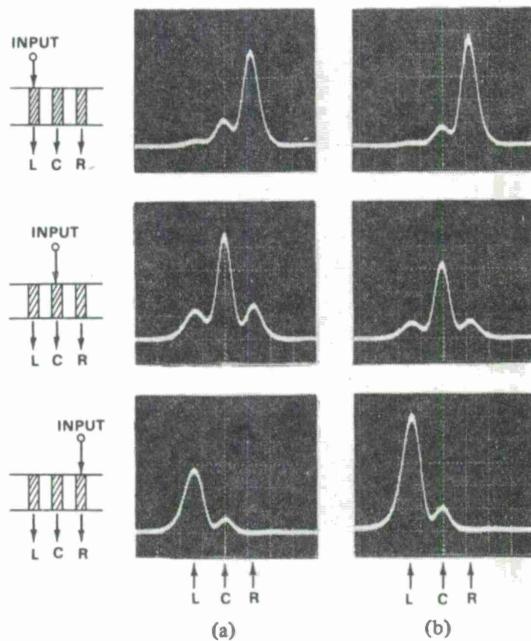
Fig. 8. A comparison of the outputs of two three-guide couplers (a) #30 and (b) #27 with power in the left outside guide, the center guide, and the right outside guide. The length of both couplers is 4.9 mm.

of both of the couplers with power input into the center guide was divided between the two outside guides. At 6.5 mm, almost all the power was transferred from one outside guide to the other for both couplers.

VI. CONCLUSIONS

Symmetrical three-guide couplers consisting of slab-coupled rib-type guides have been fabricated in GaAs. Their behavior closely approximates that predicted using an effective-index analytical method. For power into the center guide, the power is transferred symmetrically to the two outside guides in a coupling length of 3.2 mm with ≈ 1 percent of the power remaining in the center guide. The coupling length for a similar two-guide coupler is $\sqrt{2}$ times larger as predicted. For power into one of the outside guides of a three-guide coupler, the power is transferred to the other outside guide in a length of ≈ 6.4 mm, which is twice that for coupling power from the center guide to the two outside guides. In the latter case, because three modes are now involved, power transfer is not as complete as in the case where power was input into the center guide.

Symmetrical three-guide couplers of this type should prove useful as replacements for "Y"-type power dividers and combiners, especially in cases where waveguide bends would result in unacceptable losses. They may also prove useful as replacements for two-guide couplers for improved sampling and filtering (13) or where losses due to waveguide bends are unacceptable.

REFERENCES

[1] S. Somekh, E. Garmire, A. Yariv, H. L. Garvin, and R. G. Hunsperger, "Channel optical waveguide directional couplers," *Appl. Phys. Lett.*, vol. 22, pp. 46–47, Jan. 15, 1973.

[2] ——, "Channel optical waveguides and directional couplers in GaAs—Imbedded and ridged," *Appl. Opt.*, vol. 13, no. 2, pp. 327–330, Feb. 1974.

[3] J. C. Campbell, F. A. Blum, D. W. Shaw, and K. L. Lawley, "GaAs electrooptic directional-coupler switch," *Appl. Phys. Lett.*, vol. 27, no. 4, pp. 202–204, Aug. 15, 1975.

[4] F. J. Leonberger, J. P. Donnelly, and C. O. Bozler, "GaAs $p^+n^-n^+$ directional-coupler switch," *Appl. Phys. Lett.*, vol. 29, no. 10, pp. 652–654, Nov. 15, 1976.

[5] ——, "Wavelength dependence of GaAs directional couplers and electrooptic switches," *Appl. Opt.*, vol. 17, no. 14, pp. 2250–2254, July 15, 1978.

[6] J. C. Shelton, F. K. Reinhart, and R. A. Logan, "Rib waveguide switches with MOS electrooptic control for monolithic integrated optics in GaAs–Al$_x$Ga$_{1-x}$As," *Appl. Opt.*, vol. 17, no. 16, pp. 2548–2555, Aug. 15, 1978.

[7] J. C. Shelton, F. K. Reinhart, and R. A. Logan, "Characteristics of rib waveguides in AlGaAs," *J. Appl. Phys.*, vol. 50, pp. 6675–6687, Nov. 1979.

[8] A. Carenco, L. Menigaux, and P. L. Delpech, "Multiwavelength GaAs rib directional coupler switch with stepped "DB" Schottky electrodes," *J. Appl. Phys.*, vol. 50, pp. 5139–5141, Aug. 1979.

[9] A. Carenco and L. Menigaux, "GaAs homojunction rib waveguide directional coupler switch," *J. Appl. Phys.*, vol. 51, pp. 1325–1327, Mar. 1980.

[10] A. Carenco, N. T. Linh, and L. Menigaux, "InP electro-optic directional coupler," *Appl. Phys. Lett.*, vol. 40, no. 8, pp. 653–655, Apr. 15, 1982.

[11] N. L. DeMeo, F. J. Leonberger, and S. H. Groves, "Single mode GaInAsP optical waveguides," presented at the Topical Meeting of Integrated and Guided-Wave Optics, Pacific Grove, CA, Jan. 6–8, 1982.

[12] K. Iwasaki, S. Kurazono, and K. Itakuna, "The coupling of modes in three dielectric slab waveguides," *Electron. Commun. Japan*, vol. 58-C, no. 8, pp. 100–108, 1975.

[13] H. A. Haus and C. G. Fonstad, Jr., "Three-waveguide coupler for improved sampling and filtering," *IEEE J. Quantum Electron.*, vol. QE-17, pp. 2321–2325, Dec. 1981.

[14] E. A. J. Marcatili, "Slab-coupled waveguides," *Bell Syst. Tech. J.*, vol. 53, no. 4, pp. 645–674, Apr. 1974.

[15] V. Ramaswamy, "Strip-loaded film waveguide," *Bell Syst. Tech. J.*, vol. 53, no. 4, pp. 697–704, Apr. 1974.

[16] W. V. McLevige, T. Itoh, and R. Mittra, "New waveguide structures for millimeter-wave and optical integrated circuits," *IEEE Trans. Microwave Theory Tech.*, vol. MTT-23, no. 10, pp. 788–794, Oct. 1975.

[17] H. F. Taylor and A. Yariv, "Guided wave optics," *Proc. IEEE*, vol. 62, no. 8, pp. 1044–1060, Aug. 1974.

[18] M. K. Barnoski, "One-dimensional confinement," in *Introduction to Integrated Optics*, M. K. Barnoski, Ed. New York: Plenum Press, 1974, pp. 53–72.

[19] F. J. Leonberger, J. P. Donnelly, and C. O. Bozler, "Low-loss GaAs $p^+n^-n^+$ three-dimensional optical waveguides," *Appl. Phys. Lett.*, vol. 28, pp. 616–619, May 15, 1976.

[20] D. T. F. Marple, "Refractive index of GaAs," *J. Appl. Phys.*, vol. 35, pp. 124–125, Apr. 1964.

Joseph P. Donnelly (S'60–M'63) ████████ ████████████████ He received the B.E.E. degree from Manhattan College, Bronx, NY, in 1961 and the M.S. and Ph.D. degrees in electrical engineering from Carnegie-Mellon University, Pittsburgh, PA, in 1962 and 1966, respectively. His thesis work dealt with the electrical and photovoltaic properties of Ge-GaAs and Ge-Si heterojunctions grown by both liquid-phase and vapor-phase epitaxy.

From 1965 to 1966 he was a NATO Postdoctoral Fellow at Imperial College, London, England. While at Imperial College, he worked on developing a liquid-phase epitaxial system for the III-V compounds. In 1967, he joined the staff of the Massachusetts Institute of Technology, Lincoln Laboratory, Lexington, MA. At the

Lincoln Laboratory he has been concerned with the device applications of ion implantation in the III–V, II–VI, and IV–VI semiconductor compounds. In the early 1970's he worked primarily on developing ion-implantation technology for fabricating infrared detectors in the Pb-salts and InSb. More recently, his major interests have been in GaAs, InP, and related compounds. In this area he has contributed both to the development of ion-implantation technology for the III–V semiconductors and the demonstration of its use in the fabrication of a wide variety of microwave and electrooptical devices. He is currently involved in the development of laser diodes, detectors, and modulators for high-speed optical communications.

Dr. Donnelly was a National Lecturer for the IEEE Electron Devices Society in 1979. He is an Associate Member of Sigma Xi.

1970's, he worked on the evaluation of Pb-salt diode lasers and set up an optical pumping system for evaluating Pb-salt materials. He also was responsible for developing bonding and packaging techniques for HgCdTe heterodyne detection arrays. More recently, he has been involved in the evaluation of optical waveguides in InGaAsP, InP, and GaAs.

Mr. DeMeo, in addition to his technical endeavors, is responsible for most of the facilities planning for the Applied Physics Group.

*

*

Nicholas L. DeMeo, Jr. ▮▮▮▮▮▮▮▮▮ He received an Associate degree in mechanical engineering from Wentworth Institute in 1967 and a B.S. degree in industrial technology from Northeastern University, Boston, MA, in 1972.

Since joining the Applied Physics Group at the Massachusetts Institute of Technology, Lincoln Laboratory, Lexington, MA, in 1967, he has contributed to a variety of compound semiconductor device projects. In the early

Guiseppe A. Ferrante ▮▮▮▮▮▮▮▮▮▮▮▮▮. He received an electronic technician's certificate from Franklin Institute, Boston, MA, in 1961, and an Associate degree in electrical/electronic engineering from Northeastern University, Boston, MA, in 1966.

He joined the Massachusetts Institute of Technology, Lincoln Laboratory, Lexington, MA, in 1963, as a member of the Applied Physics Group, where he has contributed to various compound semiconductor device and technology development efforts. He is presently working on GaAs and InP optical waveguides.

REPORT DOCUMENTATION PAGE

1a. REPORT SECURITY CLASSIFICATION Unclassified		1b. RESTRICTIVE MARKINGS		
2a. SECURITY CLASSIFICATION AUTHORITY		3. DISTRIBUTION/AVAILABILITY OF REPORT Approved for public release; distribution unlimited.		
2b. DECLASSIFICATION/DOWNGRADING SCHEDULE				
4. PERFORMING ORGANIZATION REPORT NUMBER(S)		5. MONITORING ORGANIZATION REPORT NUMBER(S) ESD-TR-87-276		
6a. NAME OF PERFORMING ORGANIZATION Lincoln Laboratory, MIT	6b. OFFICE SYMBOL (If applicable)	7a. NAME OF MONITORING ORGANIZATION Electronic Systems Division		
6c. ADDRESS (City, State, and Zip Code) P.O. Box 73 Lexington, MA 02173-0073		7b. ADDRESS (City, State, and Zip Code) Hanscom AFB, MA 01731		
8a. NAME OF FUNDING/SPONSORING ORGANIZATION Rome Air Development Center	8b. OFFICE SYMBOL (If applicable) RADC/ESMS	9. PROCUREMENT INSTRUMENT IDENTIFICATION NUMBER F19628-85-C-0002		

8c. ADDRESS (City, State, and Zip Code) Griffiss AFB New York, NY 13440	10. SOURCE OF FUNDING NUMBERS			
	PROGRAM ELEMENT NO. 62702F, 61102F	PROJECT NO. 85	TASK NO.	WORK UNIT ACCESSION NO.

11. TITLE (Include Security Classification)

Electrooptical Devices

12. PERSONAL AUTHOR(S)
Tsang, Dean Z. and Williamson, Richard C.

13a. TYPE OF REPORT Annual Report	13b. TIME COVERED FROM 10/1/82 TO 9/30/83	14. DATE OF REPORT (Year, Month, Day) 1983, September, 30	15. PAGE COUNT 56

16. SUPPLEMENTARY NOTATION

None

17.	COSATI CODES		18. SUBJECT TERMS (Continue on reverse if necessary and identify by block number)
FIELD	GROUP	SUB-GROUP	electrooptical devices etched mirror laser buried heterostructure Q-switched diode lasers double-heterostructure GaInAsP/InP lasers

19. ABSTRACT (Continue on reverse if necessary and identify by block number)

This report covers work carried out with support of the Rome Air Development Center during the period 1 October 1982 through 30 September 1983.

A mass-transport phenomenon has been utilized to achieve GaInAsP/InP buried-heterostructure (BH) lasers. The novel technique is considerably simpler and more easily controlled than previously reported ones, and has resulted in BH lasers with threshold currents as low as 9.0 mA.

The technology for fabricating laser diodes, detectors, and optical waveguides in GaInAsP/InP epitaxial wafers requires the use of suitable etching techniques for providing smooth, damage-free surfaces for precision pattern geometries and for the preferential and reproducible removal of specific layers. It has been found that a 1 H_2SO_4:1 H_2O_2:10 H_2O room-temperature solution etches (100) $Ga_{0.27}In_{0.73}As_{0.03}P_{0.37}$ (λ = 1.3 μm) at a very constant etch rate of 1000 Å/min. Various other ratios of H_2SO_4:H_2O_2:H_2O should prove useful as slow selective etches for GaInAsP in a variety of applications.

Three-guide optical couplers consisting of slab-coupled rib-type guides have been fabricated on GaAs. Their behavior closely approximates that predicted using an effective-index analytic method. Couplers of this type should prove useful as replacements for "Y"-type power dividers and combiners, especially in cases where waveguide bends would result in unacceptable losses.

GaInAsP diode lasers with a proton-isolated modulator have been operated with full on/off modulation at rates of 3 GHz. Both the gain and loss are actively varied in the modulator in order to Q-switch the laser.

20. DISTRIBUTION/AVAILABILITY OF ABSTRACT ☐ UNCLASSIFIED/UNLIMITED ☒ SAME AS RPT. ☐ DTIC USERS	21. ABSTRACT SECURITY CLASSIFICATION Unclassified	
22a. NAME OF RESPONSIBLE INDIVIDUAL Lt. Col. Hugh L. Southall, USAF	22b. TELEPHONE (Include Area Code) (617) 981-2330	22c. OFFICE SYMBOL ESD/TML

DD FORM 1473, 84 MAR   83 APR edition may be used until exhausted.
All other editions are obsolete.   UNCLASSIFIED

SECURITY CLASSIFICATION OF THIS PAGE